SEMMELWEIS EGYETEM

DOKTORI ISKOLA

Ph.D. értekezések

3355.

BÚR ZSÓFIA

Celluláris és molekuláris élettan

című program

Programvezető: Dr. Hunyady László, egyetemi tanár

Témavezetők: Dr. Káldi Krisztina, egyetemi tanár és

Dr. Ella Krisztina, egyetemi adjunktus

TIME-RESTRICTED FEEDING PREVENTS THE DETRIMENTAL EFFECTS OF A HIGH-FAT DIET UNDER BOTH HOMEOSTATIC AND INFLAMMATORY CONDITIONS

PhD thesis

Zsófia Búr

Semmelweis University Doctoral School

Molecular Medicine Division

Supervisors: Krisztina Ella, PhD

Krisztina Káldi, MD, PhD, DSc

Official reviewers: Dávid Dóra, MD, PhD

Áron Szabó, PhD

Head of the Complex Examination Committee:

Miklós Csala, MD, PhD, DSc

Members of the Complex Examination Committee:

Csaba Bödör, PhD, DSc

László Homolya, PhD, DSc

Budapest

2025

TABLE OF CONTENTS

ABBREVIATIONS

A

ACD, allergic contact dermatitis

ACPA, anti-cyclic citrullinated peptide antibodies

ACSL1, Acyl-CoA synthetase-1

AGEP, acute generalized exanthematous pustulosis

Akt, PKB, protein kinase B

AMPK, AMP activated protein kinase

anti-CarP, anti-carbamylated protein

anti-G6PI, anti-glucose-6-phosphate isomerase

ATGL, adipose triglyceride lipase

B

bDMARD, biologic disease-modifying antirheumatic drug

BMAL1, Brain and muscle Arnt-like protein

C

CAR, CXCL12-abundant reticular cells

Ccg, clock-controlled gene

CCL2, chemokine (C-C motif) ligand 2

CD29, Integrin beta-1

CD49d, Integrin subunit alpha 4

CD62L, L-selectin

CHS, contact hypersensitivity

CK1, Casein kinase 1

CLOCK, circadian locomotor output cycles kaput

CR3, Complement receptor 3

CREB, cAMP response element binding protein

CRY, cryptochrome

CTLA4-Ig, Cytotoxic T-Lymphocyte Antigen 4 Immunoglobulin

CXCL1, C-X-C motif chemokine ligand 1

CXCL12, C-X-C motif chemokine ligand 12

CXCL2, C-X-C motif chemokine ligand 2

CXCR2, C-X-C chemokine receptor 2

CXCR4, C-X-C chemokine receptor 4

D

DBP, Albumin D-site-Binding Protein

DMARDs, disease-modifying antirheumatic drug

DNCB, 2,4-dinitrochlorobenzene

DNFB, 1-fluoro-2,4-dinitrobenzene

DSDP, delayed sleep phase disorder

E

ECM, extracellular matrix

F

FASPS, familiar advanced sleep phase syndrome

FLS, fibroblast-like synoviocyte

G

GM-CSF, Granulocyte-Macrophage Colony-Stimulating Factor

GPP, generalized pustular psoriasis

H

HF, high-fat

HPA, Hypothalamic-Pituitary-Adrenal axis

HSF1, heat shock factor protein 1

HSL, hormone-sensitive lipase

I

ICAM-1, Intracellular Adhesion Molecule 1

IL-1β, interleukin-1 beta

IL-6, interleukin-6

J

JAK, Janus kinase

K

K/BxN, KRN/B6 x NOD

KRN, Knock-in of rheumatoid node

L

LepR, Leptin receptor

LFA-1, Lymphocyte function-associated antigen 1

Lpl, lipoprotein lipase

LPS, lipopolysaccharide

LXR, Liver X receptor

M

MHC, Major histocompatibility complex

MMP, matrix metalloprotease

MS, multiple sclerosis

mTOR, mammalian target of rapamycin

N

NFIL3, Nuclear factor, interleukin 3 regulated

NLRP3, nucleotide-binding domain, leucine-rich–containing family, pyrin domain–containing-3

NSAID, Nonsteroidal Anti-inflammatory Drug

P

PBMC, peripheral blood mononuclear cell

PECAM-1, platelet endothelial cell adhesion molecule 1

Per, period

PI3K, phosphoinositide 3-kinase

PPAR, peroxisome proliferator-activated receptor

R

RA, rheumatoid arthritis

RANKL, Receptor activator of nuclear factor kappa-B ligand

Reverb, NR1D1, nuclear receptor subfamily 1 group D member 1

RF, rheumatoid factor

ROR, retinoic acid-related orphan nuclear receptor

RORE, retinoic acid-related orphan nuclear receptor responsive element

S

SLE, systemic lupus erythematosus

SNP, single-nucleotide polymorphism

T

TNFα, tumor Necrosis Factor alpha

TRE, time-restricted eating

TRF, time-restricted feeding

V

VCAM-1, Vascular Cell Adhesion Molecule 1

W

WAT, white adipose tissue

Z

ZT, Zeitgeber time

1. INTRODUCTION

1.1 CIRCADIAN RHYTHM

1.1.1 Criteria, basic parameters, and structure

The circadian rhythm plays a pivotal role in optimizing energy expenditure by adapting to daily changes of environmental cues. Multiple physiological and biochemical processes exhibit daily rhythmicity. To be classified as circadian, a rhythmic process must meet the following criteria:

- Rhythmicity persists under constant environmental conditions: For example, in constant darkness, the rhythm continues with a free-running period of approximately 24 hours.
- External cues can entrain the rhythm: Environmental factors (*e.g.* light) can reset endogenous oscillations. These synchronizers are known as *Zeitgebers*.
- Temperature compensation: While the kinetics of many biochemical processes are temperature-dependent, the speed and thus the period of circadian time measuring is maintained across a wide temperature range.

The following parameters are used to characterize the rhythm of biological responses (Figure 1). *Zeitgeber* time (ZT) refers to the time elapsed since the onset of the primary *Zeitgeber*, usually light. It is typically expressed in hours, with ZT0 marking the time of light onset. The amplitude, defined as half the difference between the maximum and minimum values of the rhythm, indicates the strength or robustness of the oscillation. For example, robust oscillations suggest a properly entrained molecular clock, while desynchronization leads to dampened amplitude of the rhythm. A commonly used parameter is the period, defined as the time between successive peaks in a cycle. The mesor (or baseline) is the mean value of the fitted curve, typically a cosine function. The acrophase refers to the time from ZT0 to the peak of the rhythm. The difference between the acrophases of two rhythms is known as a phase shift; this may manifest as a phase delay or a phase advance. Analysis of these parameters is essential for the characterization of a certain circadian oscillation.

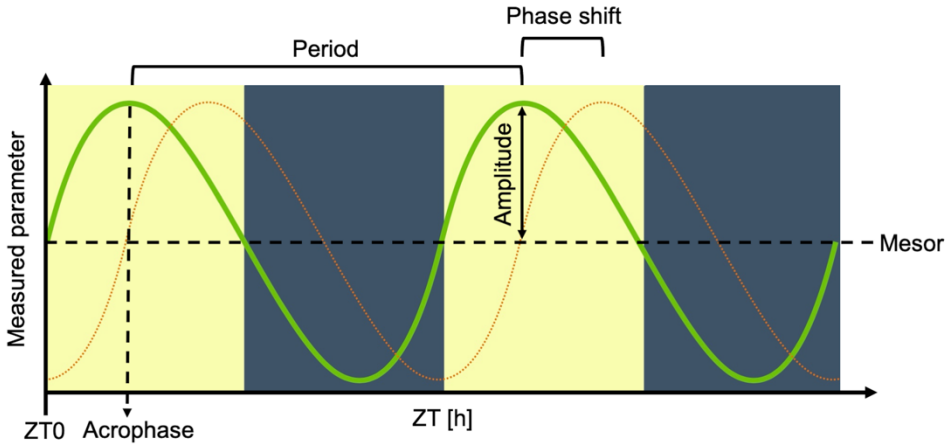

Figure 1 Circadian rhythm parameters. Amplitude, period, mesor, and acrophase are indicated. The phase shift is indicated between the green and orange curves. ZT = Zeitgeber Time. The figure is based on (1).

The circadian timekeeping system consists of input signals, an endogenous oscillator, and output signals (Figure 2). Input signals are driven by Earth's rotation on its axis and its orbit around the Sun. These regular movements result in a 24-hour light–dark cycle on Earth. Many living organisms have adapted to these daily cycles of light and temperature. As a result, activity patterns and nutrient availability also tend to follow a time-of-day-dependent rhythm. Overall, light, nutrient availability, behavioral activity, and temperature are the most common environmental cues that entrain the endogenous clock (Figure 2). Without such input signals, the free-running circadian period is approximately 24.36 hours in humans and 23.6 hours in mice (2, 3). However, *Zeitgebers* reset endogenous clocks and maintain a 24-hour rhythm.

The importance of the molecular mechanism underlying the endogenous clock was recognized with the 2017 Nobel Prize in Physiology or Medicine. It was awarded to Jeffrey C. Hall, Michael Rosbash, and Michael W. Young for their discoveries of the molecular clock in fruit flies (4-6). The functional mechanism is evolutionarily conserved across fungi, plants, and mammals. However, the structure of the clock components - except casein kinase 1 (CK1) - varies among species. To elucidate the mammalian cellular molecular clock mechanism, Figure 2 illustrates multiple transcription-translation feedback loops (7). In the nucleus, the positive core clock components, BMAL1 and CLOCK, form a complex and act as a transcription factor, binding to the E-box of promoter regions, inducing transcription of many clock genes (*period: per1, per2, per3,*

cryptochrome: cry1, cry2, reverbα, reverbβ, and *dbp)* as well as *clock-controlled genes (CCGs)*. Translation then produces PERs and CRYs, which are defined as negative factors of the clock. The PER-CRY complex associates with CK1, translocates into the nucleus, and represses the activity of the BMAL1-CLOCK complex. Posttranslational modifications such as phosphorylation and ubiquitination play a crucial role in regulating oscillation. The phosphorylation rate of clock proteins affects their stability and nuclear transport rate; hence, clock proteins are ubiquitinated and marked for degradation by the proteasome. Once the PER–CRY complex is degraded, the BMAL1-CLOCK complex initiates a new cycle.

Stabilizing loops support the function of the core loop. REVERBs inhibit, and RORs activate the RORE (retinoic acid-related orphan nuclear receptor response element) regions of genes, thereby inducing transcription of *bmal1, nfil3, and CCGs*. To further fine-tune the clockwork, DBP binds to the D-box, promoting the expression of *CCGs* and *retinoic acid-related orphan nuclear receptors: rorα, rorβ, rorγ*, whereas NFIL3 has an opposite effect.

Many *CCGs* show tissue-specific variation, and up to 80% of protein-coding genes exhibit circadian oscillations in at least one tissue (8). The molecular clock regulates several *CCGs;* therefore, various physiological functions exhibit rhythmicity. It is well established that metabolism, immune function, sleep-wake cycles, hormone levels (e.g. melatonin, cortisol), cognitive performance, DNA repair, locomotor activity, body temperature, blood pressure, and many other processes are under circadian control (9-15).

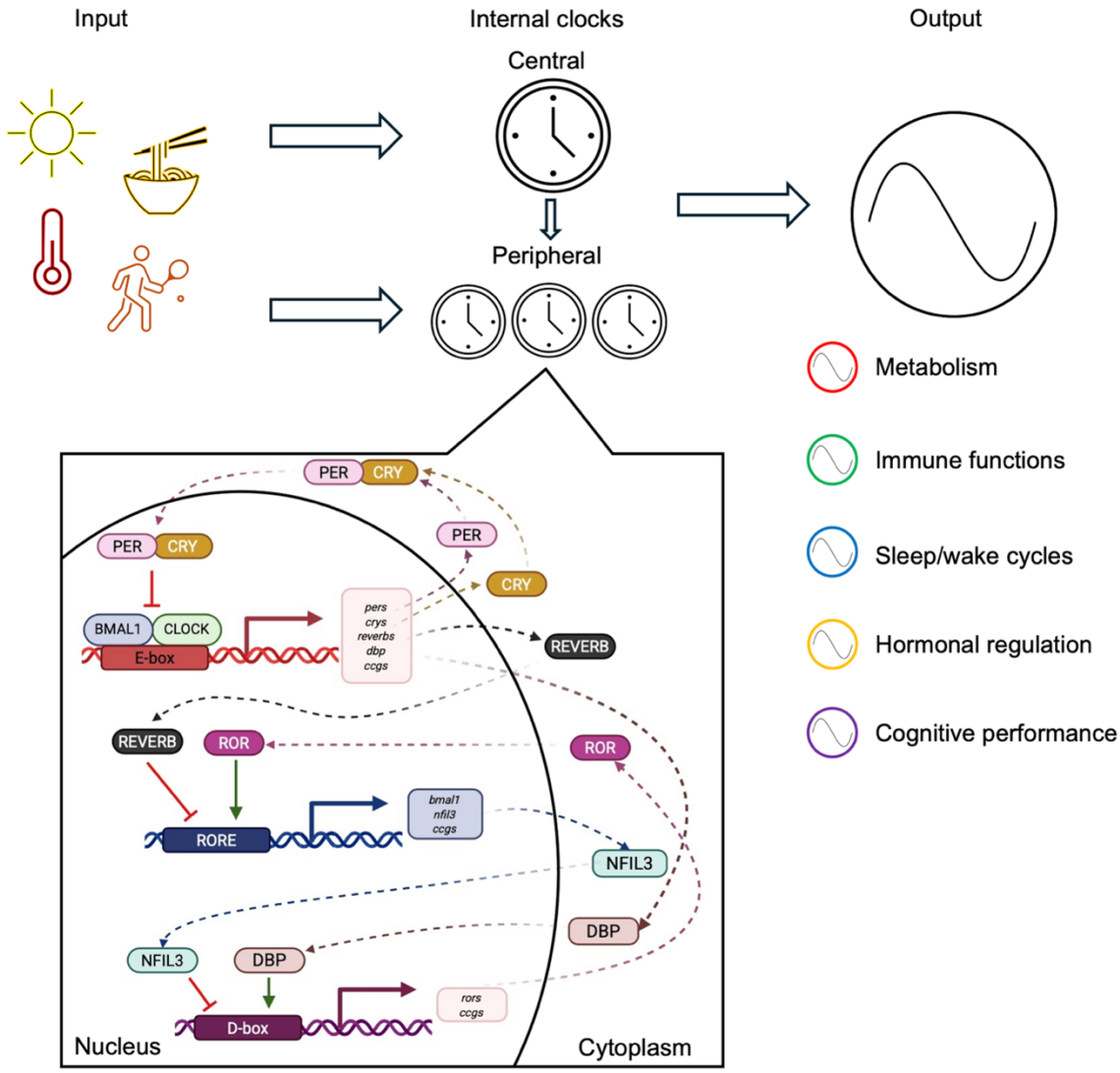

Figure 2 Structure and mechanism of the mammalian circadian system. In the cellular core loop, positive factors (BMAL1-CLOCK) induce gene expression of negative factors (per, cry). The PER-CRY complex inhibits the BMAL1-CLOCK complex, which represses transcription of the negative factors. After degradation of the PER-CRY complex, a new cycle is initiated. Stabilizing loops - based on REVERB, ROR, NFIL3, and DBP - also contribute to clock regulation. Both central and peripheral clocks are entrained by light, food availability, temperature, and activity. As outputs, several physiological processes exhibit circadian rhythmicity. The figure is based on (7). Created with BioRender.

1.1.2 Common circadian misalignments

Both intrinsic and extrinsic factors can induce circadian misalignments. Mutations in clock components are relatively rare. Human *cry1* or *per2* mutations lead to delayed sleep phase disorder (DSPD, >2 hours delay in the onset of sleep) or familial advanced sleep phase syndrome (FASPS, >2 hours advanced in the onset of sleep), respectively (16, 17). Mutations in the clock components are often associated with sleep, metabolic, and

immune function disorders (18). Furthermore, multiple circadian clock gene SNPs have been identified in human diseases, as reviewed in (19).

Conversely, majority of the modern society experiences circadian misalignments caused by external factors at some point. For instance, crossing time zones on a transatlantic flight can trigger *jetlag*, as the endogenous clock falls out of sync with the local environment. For most people, this disruption is occasional - unless their profession demands frequent travel. By contrast, individuals who have a large difference in sleep timing between workdays and free days - a phenomenon known as social *jetlag* - disrupt their circadian rhythms even every week (20). Moreover, according to 2023 European Union statistics, 18% of employees work shifts. Numerous studies have shown that shift work negatively affects well-being and longevity. Specifically, shift work has been linked to increased risks of metabolic and immune disorders, cancer, disrupted sleep-wake cycles, and mental and cardiovascular diseases (21-26).

In developed countries, extending the daily window of food access impairs feeding-fasting cycles. In parallel, the risk of metabolic disorders, such as insulin resistance and type II diabetes, is increased (27). Several studies are trying to unveil the network between metabolism and circadian rhythm. Our research group aims to analyze the interaction between food timing-dependent metabolic rhythm and immune responsiveness. The purpose of this thesis is to assess the importance of the restriction of food intake to the organism's active phase. Regarding light as the main synchronizer, all experiments were conducted under 12-hour light 12-hour dark cycles, to analyze only the effect of the feeding time and food composition. Our investigations are based on mice's feeding behavior. Under conditions with *ad libitum* food availability, food is consumed during the active phase and the beginning of the inactive phase, resulting in an approximately 14-hour feeding period (28). In our studies, beneficial effects on metabolic and immune parameters were detected when the time window of food availability was restricted to the first 10 hours of the active phase. We suggest a model with both preventive and novel therapeutic implications for inflammatory diseases.

1.2 METABOLIC RHYTHM

1.2.1 Circadian control of peripheral organs

Metabolism encompasses anabolic and catabolic processes with opposing effects on energy balance. Circadian rhythm plays a pivotal role in the temporal separation of these antagonistic processes. Mammals utilize clock-controlled adaptive mechanisms to activate the expression of anabolic hepatic enzymes, even before the expected feeding time during the active phase. Conversely, during the fasting period, which coincides with rest, catabolic processes dominate. Taken together, synchronizing the clocks of metabolic organs results in a more pronounced metabolic rhythm that contributes to the optimization of energy expenditure. To ensure metabolic functions occur at the appropriate times, multiple synchronizing signals must be integrated to coordinate the organ-specific, self-autonomous clocks. On the one hand, light cues influence the central clock located in the suprachiasmatic nucleus (SCN) of the hypothalamus. It is known that the SCN, as the master pacemaker, synchronizes peripheral clocks via neuronal, hormonal, and humoral signals. In line with this, lesioning the SCN reduces the oscillation of molecular clock components in the white adipose tissue (WAT) (29, 30).

In addition, the complex communication between peripheral organs is also critical. For example, white adipose tissue integrates signals not only from the central clock but also from other peripheral organs (31, 32). For instance, pancreatic β-cells secrete insulin in a circadian manner, which inhibits lipolysis and promotes lipogenesis in WAT during the active phase. Moreover, insulin sensitivity is influenced by the WAT clock, a mechanism referred to as clock-gating. In addition to insulin, several other peripheral signals - including ghrelin, glucagon, glucose, free fatty acids, and glucocorticoids - contribute to the rhythmic functions of adipose tissue (33).

Synchronization of metabolic organ clocks through the timing of food intake has been intensively studied over the past decade. Time-restricted food availability can entrain hepatocyte clock genes (*per1*, *per2*) even in the absence of SCN regulation (34). Timed food intake usually limits food consumption to 8–10 hours during the active phase, without caloric restriction. This approach is referred to as time-restricted feeding (TRF), the mouse model of time-restricted eating (TRE). One of the mechanisms behind TRF is that a well-defined fasting period helps counteract fed-state metabolic processes. Feeding

activates nutrient-sensing pathways and promotes anabolic processes via the insulin/PI3K/Akt/mTOR pathway. This pathway phosphorylates CK1, which in turn phosphorylates and destabilizes PER1. In contrast, fasting activates AMPK, which inhibits the mTOR pathway and promotes CRY degradation through phosphorylation. Collectively, feeding-fasting cycles enhance the amplitude of clock gene expression. In parallel with these mechanisms, several other nutrient-sensing pathways interact with clock components to fine-tune metabolic rhythms in response to nutrient availability and cellular energy demand (35).

It is well established that TRF helps to prevent obesity. The general mechanism underlying time-restricted feeding has been further investigated by Hepler and colleagues, who demonstrated that TRF reduces obesity by activating futile creatine cycling in adipocytes and enhancing thermogenesis (36). This mechanism also explains how TRF can reduce or stabilize body weight - depending on the duration of the feeding window - even without caloric restriction.

Nowadays, multiple clinical trials have investigated the beneficial effects of TRE, both with and without caloric restriction. These studies focus on the prevention and treatment of prediabetes, type II diabetes, metabolic syndrome, bipolar disorder, cancer-related persistent fatigue, and bone metabolism (37-43). TRF or TRE likely has beneficial effects in inflammatory diseases, although research in this area remains limited.

In addition to food timing, nutrient composition also affects metabolic clocks. For example, a high-fat (HF) diet was shown to disrupt clock gene expression in both the liver and WAT (44). High-fat chow is often used in diet-induced obesity models. In most studies in the literature, the HF diet period lasts for 8 to 12 weeks and leads to significant obesity. Both immune and metabolic parameters are significantly impaired under this condition compared to normal chow feeding. Calorie-rich HF diet increases blood glucose levels, worsens insulin sensitivity, and elevates serum leptin and cytokine levels which are all indicators of low-grade inflammation (28). Relatively long-term effects of a HF diet are already well-characterized, and the diet develops a moderately severe metabolic disturbance. In turn, a short-term HF diet could acutely disturb the metabolic state, offering an opportunity to investigate obesity-independent effects of a HF diet on the

WAT clockwork. Our investigations also address how metabolic state and immune responsiveness are influenced by a short-term (4-week) HF diet.

1.2.2 Rhythmic function of white adipose tissue

Integration of central and peripheral signals and self-autonomous adipocyte clock maintains the homeostatic functions of white adipose tissue (WAT). Depending on the WAT depot, different profiles have been characterized (due to differences in innervation, vascularization, and gene expression patterns) (45). For clarity, I would predominantly focus on the rhythmic functions of visceral white adipose tissue. Beyond its role in energy storage, WAT also acts as an endocrine organ secreting adipokines, influencing insulin sensitivity, and participating in inflammatory processes as well.

Let us review some circadian-controlled genes whose main function is associated with energy storage. *Atgl (Adipose triglyceride lipase)* and *Hsl (hormone-sensitive lipase)* genes are clock-controlled genes and play a key role in lipolysis. Furthermore, many anabolic genes show diurnal variations, like *Acsl1(Acyl-CoA synthetase-1)* and *Lpl (lipoprotein lipase)* (33). A recent study showed that *de novo* lipogenesis is supported by rhythmic IL-17 production by γδ T cells (46), revealing the close connection between energy stores and immune functions.

Besides, WAT is an endocrine organ, secreting both hormones and pro-inflammatory adipokines, such as leptin, visfatin, resistin, chemerin, omentin, and chemokines/cytokines like CCL2, IL-1β, IL-18, IL-6, TNFα, and many others, negatively affecting immunometabolic-related diseases (47). The anti-inflammatory adipokines are adiponectin, apelin and IL-10. A high adiponectin level is connected with enhanced insulin sensitivity and is considered a positive biomarker in metabolic health (47). Adipose tissue's clock components (*e.g.* REVERB), adipokines, or metabolic stress signals affect the NF-κB pathway, which promotes the transcription of *tnfa*, *nlrp3, pro-il-18* and *pro-il-1β* (Figure 3). Upon secondary activation signal, NLRP3 inflammasome activity results in the cleavage of pro-IL18 and pro-IL-1β by caspase-1 (Figure 3) which control pro-inflammatory processes, such as promoting M1 macrophage polarization.

.

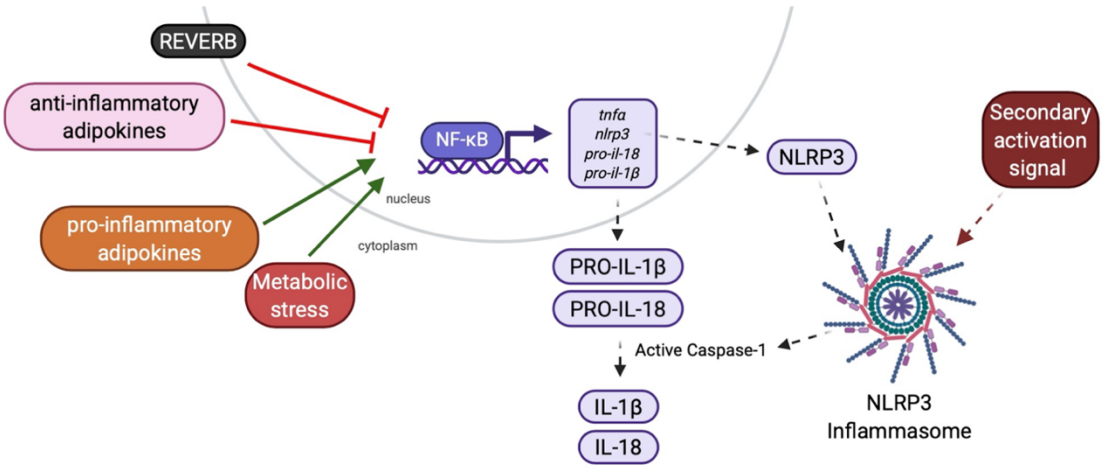

Figure 3 Regulation of the NF-κB pathway and NLRP3 inflammasome in white adipose tissue. Adipokines, REVERB, and metabolic stress signals indirectly modulate NF-κB activity, inducing transcription of tnfα, nlrp3, pro-il-18, and pro-il-1β. NLRP3 activation then results in the activation of caspase-1, which catalyzes the cleavage of pro-IL-18 and pro-IL-1β into their active forms. The figure is based on (48). Created with BioRender.

Our main goal was to investigate leptin, as it is a direct output of the clock, showing oscillation in both WAT and the serum (49). Therefore, leptin action likely occurs in a time-dependent manner under homeostatic conditions. In addition to leptin production, several other immunometabolic functions of WAT have been recognized over the last decades, highlighting the close link between immune activity in WAT and the metabolic status of the organism (50-54).

1.3 TEMPORAL REGULATION OF IMMUNE RESPONSIVENESS

1.3.1 Time-of-day-dependent leukocyte rhythm

The common assumption that alignment of the circadian rhythm has an anti-inflammatory effect is overly simplistic (to the reader: circadian researchers would never simplify it that much!). In reality, circadian rhythm controls the immune system in a time-dependent manner: it enhances leukocyte trafficking during the active phase to ensure immune readiness in organs and tissues, when the likelihood of pathogen exposure is higher. In contrast, during the inactive phase, the clock supports leukocyte homing and thus the clearance of senescent cells, leading to prevention of immune overactivation and autoimmune responses. Essentially, the circadian clock balances the “two faces” of the immune system: due to the daily activity rhythm, infection risk is elevated during active

hours, while during sleep - when exposure to pathogens is minimal - phagocytosis of aged immune cells is more prominent (55). Both in humans and animals, leukocyte count in peripheral blood shows robust rhythmicity (56). *Bmal1* deficiency abolishes this rhythm, which strongly supports circadian regulation (57).

1.3.2 Circadian patterns in neutrophil function

My work was especially focused on the neutrophil's role in different immune responses and its interaction with the circadian regulation. Our research group hypothesized that changing the rhythm of food intake and a high-fat diet significantly impacts neutrophil responsiveness and immune surveillance.

To place this study into context, it is essential to first review the literature on neutrophil rhythms and their regulation. At the beginning of the active phase, bone marrow neutrophils ($CXCR2^{hi}$, $CD62L^{hi}$, $CXCR4^{low}$, microvilli-dense surface) egress into the bloodstream (so-called 'fresh' neutrophils) to reach target organs via rolling, adhesion, and diapedesis. Local adhesion molecules on the endothelium (VCAM-1, ICAM-1, ICAM-2, P-selectin and E-selectin) are rhythmically expressed in an organ-specific manner, resulting in a circadian manner of leukocyte migration (58-61). Later on, neutrophils exhibit decreased CD62L and CXCR2, while CXCR4 expression increases. Concomitantly with the maturation, integrin expressions, like CD11a, CD49d, and CD29 are also elevated. Next, the aged neutrophils ($CXCR2^{low}$, $CD62L^{low}$, $CXCR4^{hi}$, with a microvilli-deficient surface) migrate into naïve, homeostatic tissues to undergo non-canonical functions (62). For instance, neutrophils contribute to the rhythmic expression, transportation of extracellular matrix (ECM) proteins, as well as the remodelling of ECM, such as TGFß-dependent physical shield formation in the skin (63). In the inactive phase, neutrophil clearance is facilitated by CXCL12-abundant reticulocyte (CAR) cells; CXCL12 is the main retention factor in the bone marrow. Senescent cells are phagocytosed by macrophages, leading to LXR activation in these cells, which in turn modulates the bone marrow niche. Specifically, activation of LXR suppresses CXCL12 production by CAR cells (55, 64). Conversely, neutrophil egress is promoted by CXCL1 and CXCL2 chemokines (62). Notably, *cxcl2* is a *CCG* in neutrophils, allowing autocrine regulation of neutrophils through CXCR2 signaling (60). During inflammation, elevated tissue levels of CXCL2 (as a chemotactic factor) promote neutrophil recruitment, and

CXCR2 signaling activates NLRP3 inflammasome, which is a hallmark of IL-1ß release (65). We aimed to investigate how TRF and high-fat diet affect peripheral blood leukocyte rhythm and the expression of adhesion molecules on the surface of myeloid cells (priming). Furthermore, to assess migratory capacity in different feeding groups, we applied autoimmune disease models as well.

1.3.3. Expression of adhesion molecules and chemokine receptors is under circadian control

Neutrophils show rhythmic expression of CD62L, CD11a, CXCR2, CXCR4, CD49d, and CD29 (59), which also brings them within the scope of our investigation. We demonstrated that TRF decreases the expression of adhesion molecules and chemokine receptors on the surface of myeloid cells under steady-state conditions (66) (Table 1). However, the mechanism resulting in less responsive neutrophils under TRF remains unexplored.

Table 1. TRF decreases the expression of adhesion molecules and chemokine receptor on the surface of the myeloid cells (66).

Adhesion molecule/ chemokine receptor	**Function**	**TRF effects on neutrophils**	**TRF effects on monocytes**
CD62L	L-selectin, rolling	↓	-
CD11a	Integrin subunit of LFA-1, adhesion	-	-
CXCR2	Chemokine receptor, activation	-	no data
CXCR4	Chemokine receptor, activation	↓	↓
CD49d	Integrin subunit of VLA-4, adhesion	↓	↓
CD29	Integrin subunit of VLA-4, adhesion	-	↓

1.4 AUTOIMMUNE AND INFLAMMATORY DISEASES

1.4.1 Rheumatoid arthritis

The worldwide prevalence of Rheumatoid Arthritis (RA) is estimated at 0.24%; however, it is higher in Europe and North America, 0.6-1% (67). In addition, the lifetime risk of RA is higher in women (3.6%) compared with men (1.7%) (68). RA is a multifactorial,

autoimmune, and systemic disease characterized by painful joint stiffness and swelling. RA is a chronic disease with periodically recurring acute flares. The development of RA is typically described as occurring in genetically predisposed individuals, in whom environmental factors (*e.g.*, smoking) trigger post-translational protein modifications, such as citrullination, carbamylation, and acetylation. Autoantibodies subsequently target these modified proteins. When rheumatoid factor (RF), anti-carbamylated protein (anti-CarP), and anti-cyclic citrullinated peptide antibodies (ACPA) are present, RA is classified as seropositive (69). These antibodies can already be detected prior to the onset of the symptoms. The antibodies bind to synovial surface molecules, forming immune complexes consistent with type III hypersensitivity. In addition, intense leukocyte infiltration occurs in the synovium and synovial fluid. Both innate and adaptive immune responses are activated, with secretion of numerous cytokines and chemokines (IL-1β, TNFα, IL-6, GM-CSF, RANKL, IL-17, CCL2, CXCL1, CXCL2), which further recruit immune cells (Figure 4). IL-1β, TNFα, and IL-6 levels exhibit circadian variation (70); and these mediators regulate the daily changes in osteoclast activity, matrix metalloprotease (MMP) production by fibroblast-like synoviocytes (FLS) (71), and recruitment of the immune cells (Figure 4). Overall, RA reprograms FLS and other involved cells, leading to arthritic symptoms that follow a circadian rhythm. In humans, symptom severity typically peaks in the early morning and wanes by the afternoon (70).

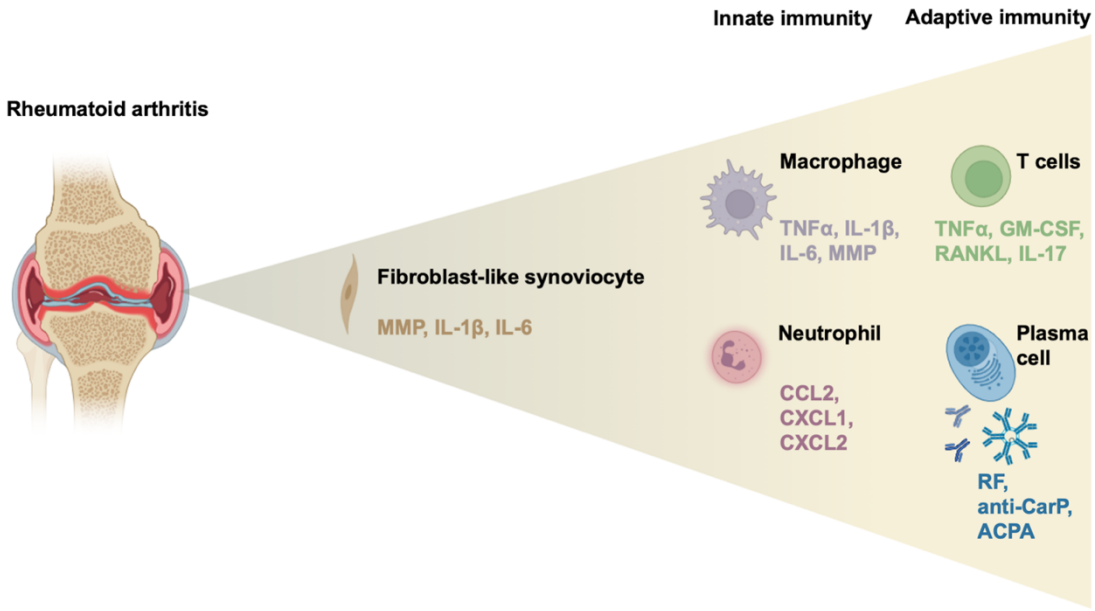

Figure 4. Overactivation of both innate and adaptive immunity exacerbates autoimmune rheumatoid arthritis. Alongside immune cells, cytokine production, fibroblast-like synoviocytes secrete matrix metalloproteases (MMP), IL-1β, and IL-6, further amplifying the immune response. The figure is based on (72). Created with BioRender.

1.4.2 Mouse models of rheumatoid arthritis

Various mouse arthritis models have been developed, including antigen-, proteoglycan-, oil-induced arthritis, streptococcal cell-wall arthritis, collagen-induced arthritis (CIA), and K/BxN serum transfer arthritis (STA). Among these, CIA and STA are the most commonly used models to investigate arthritis pathogenesis. CIA is a chronic inflammatory disease model induced by type II collagen emulsified in Freund's adjuvant (73). Notably, previous studies have shown that HF diet worsens CIA rheumatic scores without affecting body weight (74). To elucidate the effect of feeding regimens on the severity and timing of arthritis flares, we used the K/BxN STA model - an acute-phase experimental model of human RA. Arthritic serum, collected from T cell receptor transgenic KRN and MHC class II allele Ag7 mice, contains autoantibodies targeting glucose-6-phosphate isomerase (anti-G6PI autoantibodies) (75), which trigger joint inflammation in the limbs. In this model, myeloid cells serve as key effector cells, yet the disease does not develop in the absence of adipsin (also known as complement factor D) (76) or adaptive immunity (77). Similar to human RA, the K/BxN STA model reveals a wide array of inflammatory mediators. C5a binds to its receptor C5aR on neutrophils, leading to the release of leukotriene B4 (LTB4) and IL-1β, and inducing the secretion of chemoattractants, including CXCL1, CXCL2, CXCL5, CCL3, and CCL9. The integrin

LFA-1 of the immune cells binds to ICAM-1, ICAM-2, and JAM-A, expressed on the vascular endothelium (78), resulting in the recruitment of leukocytes to the synovial fluid, consequently exacerbating arthritis severity.

1.4.3 Therapeutic approaches for rheumatoid arthritis

Clinicians monitor the severity of symptoms using the standardized rheumatoid arthritis activity score. The main goal of the therapy is to prolong the remission phase and/or reduce disease activity. Several drugs are offered for RA treatment, such as NSAIDs (non-steroidal anti-inflammatory drugs), which lack disease-modifying activity, but play an important role in relieving joint pain even during diagnostic evaluations. A broad drug repertoire is available; for instance, meloxicam (a non-selective COX inhibitor) and celecoxib (a selective COX-2 inhibitor) are indicated for mild RA. According to current RA treatment guidelines, nonbiologic DMARDs (disease-modifying anti-rheumatic drugs) are the first-line medicines, including methotrexate (MTX), hydroxychloroquine, sulfasalazine, azathioprine, cyclophosphamide, and leflunomide. MTX is generally administered in combination with hydroxychloroquine, sulfasalazine, and, in special cases, with azathioprine, cyclophosphamide. Leflunomide is considered a substitute medication for MTX (79). When nonbiologic DMARDs fail or cause intolerable side effects, biologic DMARDs (bDMARDs) are introduced as second-line therapeutic options. These highly effective agents target immune response pathways, inflammation, pannus formation, and bone erosion. This class includes anti-TNFα antagonists (etanercept, infliximab, adalimumab, golimumab, certolizumab pegol) anti-IL-6 antagonists (tocilizumab, sarilumab), IL-1 antagonists (anakinra, canakinumab) T–cell costimulation inhibitor (abatacept CTLA4-Ig), anti-CD20 monoclonal antibody that depletes B cells (rituximab), JAK (JAK1, JAK3) inhibitors (tofacitinib, baricitinib, upadacitinib) (79). However, patients may become non-responders, lose responsiveness, develop intolerable side effects, or the severity of side effects can outweigh the therapeutic benefit. A hurdle of the biologic therapies is the increased risk of infections, which necessitates temporary treatment discontinuation during active infections.

In combination with DMARDs and biologics, corticosteroids, including prednisolone and methylprednisolone are used in RA management (79). However, long-term steroid use can disrupt the hypothalamic-pituitary-adrenal (HPA) axis, suppressing endogenous

cortisol production. These agents can be administered as short-term pulse therapy or as daily regimens, providing immunosuppression and anti-inflammatory effects. Given that pro-inflammatory cytokine levels peak during the night, modified-release, low-dose prednisone was developed to enhance efficacy at night and minimize adverse effects. Overall, this innovation represents a promising strategy for chronotherapy in the context of RA management (80, 81).

1.4.4 Allergic contact dermatitis and pustulosis

Allergic contact dermatitis (ACD) affects approximately 20% of the broader population to at least one contact allergen (82). ACD is a delayed-type (type IV) hypersensitivity reaction. In the sensitization phase, an offending agent or a hapten (typically a small molecule <500 Da) covalently binds to a larger carrier protein and forms an immunogenic complex (83). The allergen is taken up and presented by Langerhans cells (LCs, specialized epidermal dendritic cells). LCs migrate to the regional lymph nodes, interact with naïve T cells, and thereby induce their activation and clonal expansion. These antigen-specific T cells later migrate to the epidermis and persist as tissue-resident memory T cells. In the elicitation phase, re-exposure to the allergen triggers recognition of the antigen by memory T cells, leading to a rapid and local inflammatory response. DC cells produce IL-23, promoting Th17 differentiation, which in turn secrete IL-17 (84, 85). Via IL-17 receptor signaling, keratinocytes release cytokines and chemokines that orchestrate innate and adaptive immune responses. This includes promoting immune cell recruitment and the production of antimicrobial peptides, matrix proteins, and chemoattractants (e.g., CXCL8, IL-1, IL-6, and TNFα). Accumulated immune cells, such as neutrophils, monocytes, and macrophages, further amplify the inflammation by secreting CXCL1, CXCL2, and IL-1β (86, 87). The fundamental role of IL-17 (88) and neutrophils (89) has been confirmed in murine ACD models, both being essential for the development of the characteristic skin reaction.

Moreover, the intensity of the inflammation exhibits a circadian pattern: exposure during the active phase elevates macroscopic and cellular inflammatory responses compared to exposure during the resting (inactive) phase (90). In addition, clock mutant mice exacerbate cutaneous inflammatory processes (91), highlighting the circadian control of allergic contact dermatitis.

ACD and psoriasis are distinct in etiology but share similarities in cytokine profiles (particularly IL-23/IL-17 axis and TNFα) and T cell-driven (Th17, Th1) immune response (92). A rare, severe subtype known as generalized pustular psoriasis (GPP), is characterized by dysregulation of the IL-36 signaling pathway. This leads to keratinocyte-mediated release of neutrophil-attracting chemokines (e.g., CXCL1, CXCL2), driving robust neutrophil infiltration into the epidermis, forming sterile pustules (93). Additionally, acute generalized exanthematous pustulosis (AGEP) shares histological similarities with GPP, including prominent intraepidermal pustule formation and neutrophilia; though AGEP is typically drug-induced and self-limiting (94).

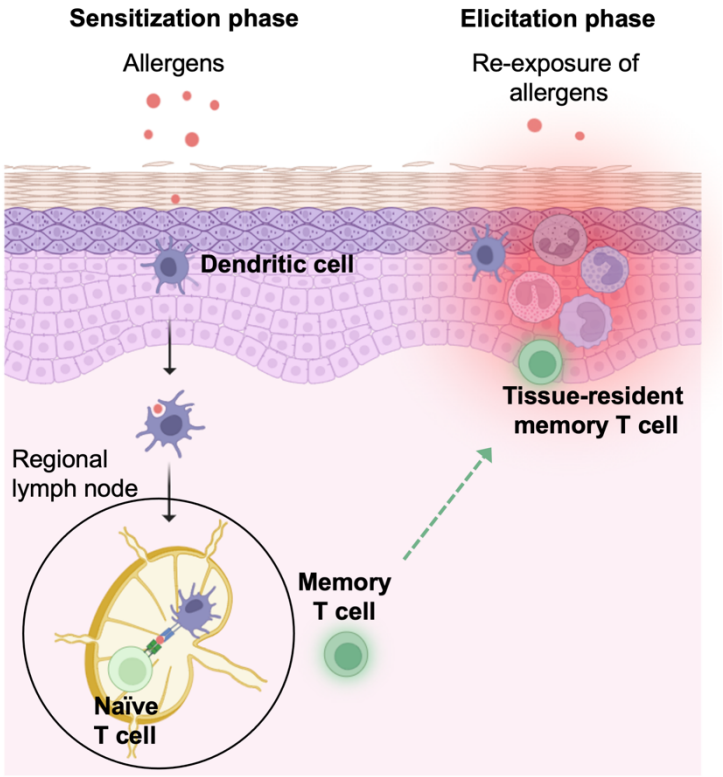

Figure 5 Sensitization and elicitation in contact hypersensitivity. The initial allergen encounter is clinically silent. Allergens are captured by dendritic cells, and presented to naïve T cells via MHC molecules. Following clonal expansion, effector T cells differentiate, and some become tissue-resident memory T cells within the skin. Upon re-exposure, the allergen elicits a rapid immune response involving tissue-resident T cells, keratinocytes, and dendritic cells, leading to cytokine and chemokine release, further promoting immune cell recruitment. The figure is based on (95). Created with BioRender.

1.4.5 Skin inflammatory mouse models

Contact hypersensitivity (CHS), a widely used mouse model of allergic contact dermatitis, is commonly induced by topical application of contact allergens, such as oxazolone, TNCB (2,4,6-trinitrochlorobenzene), DNCB (2,4-dinitrochlorobenzene), DNFB (1-fluoro-2,4-dinitrobenzene), ovalbumin, FITC, and croton oil, all of which have been extensively characterized in preclinical studies (96). In these models, two distinct phases are defined: sensitization and elicitation. Omission of the sensitization phase may model irritant contact dermatitis instead. During the sensitization phase, a relatively high concentration and volume of allergen is applied to the shaved abdomen or ear. Five to six days later, elicitation is triggered using a lower amount of the allergen, usually applied to the ears. CHS severity is commonly evaluated by measuring ear thickness, which typically peaks 24 to 48 hours post-challenge, depending on the experimental setup. Inflammation usually resolves within a few days after reaching its peak. Furthermore, as demonstrated by Röse et al., repeated allergen exposure can model chronic inflammatory dermatitis. Based on the application schedule, acute, subacute, and chronic CHS models have been developed to induce psoriasis-like skin inflammation (97).

1.4.6 Therapeutic approaches for skin inflammatory conditions

According to therapeutic guideline for ACD, the primary step is to identify and eliminate the allergen from the patient's environment. If complete avoidance is not feasible, appropriate therapeutic strategies must be considered. When less than 20% of the body surface is affected, topical corticosteroids remain the first-line treatment. For more widespread involvement, systemic corticosteroids are considered first-line therapy. However, long-term steroid use is associated with side effects, such as skin thinning. In more severe or refractory cases, alternative agents - including tacrolimus, mycophenolate mofetil or cyclosporin - may be employed. In contrast, corticosteroids are generally avoided in the treatment of generalized pustular psoriasis (GPP), as withdrawal can trigger or exacerbate the condition. Instead, first-line therapies for GPP include acitretin, cyclosporin, MTX, and TNFα antagonists (93).

Overall, the role of dietary interventions in enhancing the efficacy of existing therapies for ACD, psoriasis, and RA remains elusive, highlighting the need for further

investigation, especially in light of emerging links between metabolic rhythms and immune functions.

1.5 LEPTIN AND ITS RECEPTORS: POTENTIAL LINK BETWEEN METABOLIC RHYTHM AND IMMUNE FUNCTIONS

As mentioned previously, leptin is a *CCG* in WAT and serum leptin levels proportionally correlate with white adipose tissue mass and exhibit circadian rhythmicity. In mice, leptin levels peak during the night and are at a trough around midday. Leptin exerts pleiotropic effects, influencing insulin secretion, fertility, bone density, angiogenesis, thermogenesis, and immune responses (98). In addition, leptin is the main satiety hormone, which, via acting on POMC neurons through the ObRb receptor, decreases food intake. Indeed, in central leptin resistance, systemic leptin levels are elevated, and the anorexigenic effect is impaired. Notably, high-fat-fed animals exhibit resistance to leptin's appetite-suppressing function, while peripheral leptin signaling remains intact. Leptin promotes CXCL1 and TNFα secretion by macrophages and enhances neutrophil activity (99).

While leptin signaling is primarily mediated by the long isoform (ObRb) of leptin receptor (LepR), short isoforms (ObRa, ObRc, ObRd, ObRf) may also contribute to leptin's biological effects (Figure 6). The soluble isoform (ObRe) is not involved in signal transduction but may influence leptin action by modulating its availability and distribution (100). LepRs belong to the class I cytokine receptor family (alongside the IL-6 receptor), sharing identical extracellular protein motifs (N-terminal domain, two cytokine receptor homology modules, fibronectin type III, and immunoglobulin domain). The isoforms differ in their intracellular domains. The cytosolic part of ObRb has two box domains and three tyrosine residues, whereas the short forms have only two box domains. The soluble isoform is generated by the shedding of the extracellular domain. The intracellular structure defines downstream signaling. ObRb primarily signals through the JAK2/STAT3 pathway, but also activates PI3K/Akt/mTOR and MAPK pathways. In contrast, the short forms are mainly linked to MAPK signaling (100). LepRs are expressed by multiple peripheral organs, tissues, and cells, including those with immune function. For instance, in mesenchymal stromal cells of the bone marrow, leptin regulates *cxcl12* expression via ObRb (101, 102). In T cells, leptin promotes naïve CD4+ T cell differentiation into Th1/Th17 cells and inhibits Treg cells' proliferation through ObRb

(100, 103). Consequently, leptin deficiency is associated with elevated susceptibility to infections, whereas high leptin levels promote autoimmune processes. Leptin, probably acting via ObRa, triggers upregulation of CD11b on human neutrophils (104). Monocytes express both ObRa and ObRb, mediating the production of inflammatory cytokines (105).

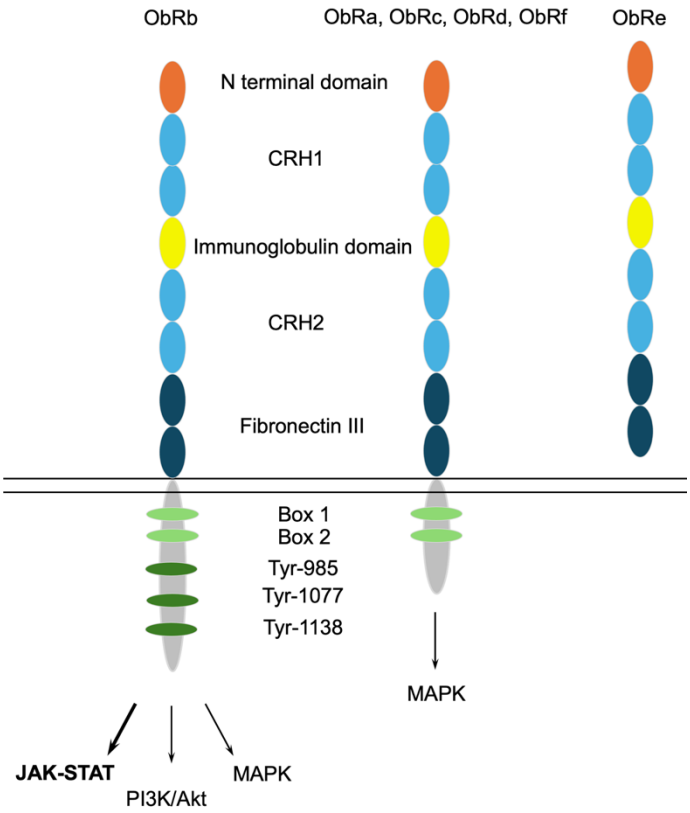

Figure 6 Structures and signaling pathways of leptin receptors. The extracellular region of leptin receptors consists of an N-terminal domain, two cytokine receptor homology regions (CRH1 and CRH2), an immunoglobulin-like domain, and a fibronectin type III domain. The intracellular domain of the long form (ObRb) contains Box1, Box2, and three tyrosine residues and primarily signals through the JAK-STAT pathway. In contrast, the short isoforms (ObRa, ObRc, ObRd, ObRf) possess only Box1 and Box2, and might activate MAPK signaling. The figure is based on (100).

A key insight into leptin signaling came from the discovery of a novel diabetic mutation in a mouse in 1966 by D. L. Coleman and his colleagues (106). This point mutation of ObRb isoform defines the *db/db* mouse strain (107), which has been applied as an obesity and diabetes model due to the lack of negative feedback in appetite control. *Db/db* mice have severe symptoms, including glycosuria, hyperglycemia, hyperinsulinemia, obesity, polyphagia, polyuria, polydipsia, and proteinuria. Serum leptin levels are 50-fold higher in *db/db* than in wild-type animals. Importantly, ObRb may form heterodimers with short-

form leptin receptors (108). Mutant ObRb disrupts leptin signaling, and ObRb might be replaced by the short form of leptin receptors. Overall, the *db/db* mouse model is well-suited for studying how elevated leptin levels influence immune responsiveness via the short-form of leptin receptor. However, it is also important to consider the limitation that obesity itself promotes low-grade inflammation and the production of multiple pro-inflammatory mediators.

Leptin acts as a key metabolic hormone that communicates the body's energy status to peripheral tissues, including immune cells. We hypothesize that timed food intake combined with a high-fat diet may modulate immune responses by altering the production and rhythmic secretion of leptin from white adipose tissue. Moreover, disrupted leptin signaling is associated with enhanced pro-inflammatory responses, prompting growing interest in the association between circulating leptin levels and inflammation severity. Animal models provide compelling evidence supporting leptin's immunomodulatory role: leptin deficiency inhibits the induction and progression of disease in mouse models of multiple sclerosis (MS) (109) and reduces autoantibody production in systemic lupus erythematosus (SLE) models (110, 111). Conversely, exogenous leptin administration restores disease susceptibility in leptin deficiency and exacerbates MS and SLE severity by enhancing T cell responses in wild-type animals (112-117).

Studies have assessed multiple variables, including body weight, circulating leptin levels, immunological markers, disease severity, and metabolic parameters. Although these findings primarily concern adaptive immunity, the contribution of innate immune pathways remains underexplored. Our aim is to elucidate how timed food intake shapes immune responsiveness and to uncover the mechanistic link between leptin signaling and inflammatory processes.

2. OBJECTIVES

Disrupted feeding schedules and high-fat diet contribute to the development of metabolic disorders, including obesity and diabetes. Conversely, time-restricted feeding (TRF) has emerged as a well-tolerated and sustainable strategy for the prevention and management of these conditions. Given the close connection between metabolism and immunity, our aim was to investigate the impact of a 4-week TRF on metabolic and immune parameters under steady-state conditions. Furthermore, we aimed to explore how TRF influences the progression of (1) K/BxN serum-transfer arthritis, a murine model of human rheumatoid arthritis, and (2) contact hypersensitivity, a mouse model for allergic contact dermatitis.

Our study aimed to address the following questions:

1. What are the effects of normal versus high-fat diets on metabolic parameters, and does the timing of food intake influence key indicators of the metabolic state?
2. How are the inflammatory mediators and clock gene expressions modulated in white adipose tissue by different feeding regimens?
3. Does a high-fat diet alter neutrophil and monocyte activation under steady-state conditions? Is adhesion molecule expression affected by TRF?
4. Can TRF mitigate the severity of inflammatory arthritis despite a high-fat diet?
5. Which immune parameters are influenced by a high-fat diet during a contact hypersensitivity reaction? How does time-restricted feeding attenuate CHS response?

3. MATERIALS AND METHODS

3.1 ANIMALS AND DIETS

In our experiments male C57BL/6N (B6 *wild type*) and BKS.Cg-Dock7m$^{+/+}$Leprdb/J ObRb leptin receptor mutant (*db/db*) mice and their *wild type* (*wt*) controls with BKS background were used. The animals were maintained in a minimal disease animal facility under 12-hour light and 12-hour dark cycles and fed with standard chow diet. At the age of 60-80 B6 *wild type* mice were randomly assigned to a calorie-dense high-fat diet (HF, high-fat, cat.no.: D12230, fat content: 59%) or standard diet (NC, normal chow, cat.no.: S8189, fat content: 17%). Each dietary group was further divided into two feeding regimens: *ad libitum* (AL) and time-restricted feeding (TRF). In the TRF group food availability was restricted to the first 10 hours of the active phase of the animals (Figure 7).

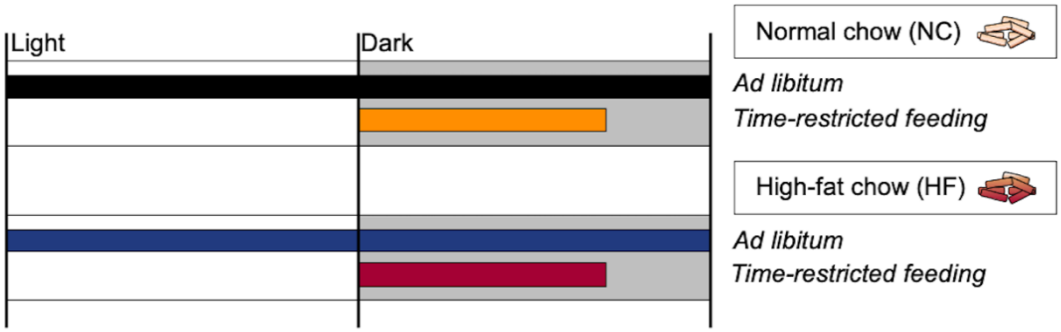

Figure 7. Schematic outline of the feeding regimes. Mice were fed either normal chow (NC) or high-fat (HF) chow. Ad libitum (AL) fed groups had constant food access, whereas time-restricted feeding (TRF) was limited to the first 10 hours of the active phase of the animals.

During conditioning, caloric intake and body weight were monitored weekly. Experiments were conducted after a 4-week conditioning period. Indeed, feeding schedules were maintained until the end of the experiments. Study design and experimental procedures were approved by the Animal Experimentation Review Board of Semmelweis University and the Government Office for Pest County (Hungary) (Ethical approvals: PE/EA/1967-2/2017 (KA-2281) and PE/EA/00375-6/2024.

3.2 INTRAPERITONEAL GLUCOSE TOLERANCE TEST

Mice were fasted 16 hours before the intraperitoneal glucose tolerance test (IPGTT). 1 g glucose/kg body weight dose was injected at ZT14. Baseline fasting glucose, and blood

glucose levels 15, 30, 60, 90, 120 min after glucose administration were measured with Dcont Trend glucose meter. Due to the fasting period and glucose challenge, these animals were excluded from further investigations.

3.3 GENE EXPRESSION ANALYSIS OF WHITE ADIPOSE TISSUE

Epididymal white adipose tissue was collected at different time points: ZT1, ZT5, ZT9, ZT13, ZT17, and ZT21, respectively. Samples were frozen in liquid nitrogen, and RNA isolation was conducted using TRI reagent (Sigma-Aldrich). cDNA was synthesized using the QuantiTect® Reverse Transcription Kit (Qiagen) following the manufacturer's instructions. Relative expression levels of *dbp, per1, per3, tnfα, il1β, il18, nlrp3, leptin,* and *adipsin* were measured in a Light Cycler® 480 system (Roche) using TaqMan hydrolysis probes (Table 2). *rplp0* was used as a reference. The second derivate maximum method was applied for gene expression analysis in LightCycler® Relative Quantification Software (version 1.5.0.39, Roche).

Table 2. Primer and probe sequences for gene expression analysis.

Gene		Sequence
rplp0	Forward	5'-CTCGCTTTCTGGAGGGTGTC-3'
	Reverse	5'-AGTCTCCACAGACAATGCCA-3'
	Probe	5'FAM-TGCCTCGGTGCCACACTCCA-TAMRA3'
dbp	Forward	5'- CCATGAGACTTTTGACCCTCG-3'
	Reverse	5'- TCATTGTTCTTGTACCTCCGG-3'
	Probe	5'FAM-CACCTGGACTTTCCTTGCCTTCTTCA-TAMRA3'
per1	Forward	5'-TGTGTCAAGCAGGTTCAGG-3'
	Reverse	5'-TGTCCTGGTTTCGAAGTGTG-3'
	Probe	5'FAM-AGTGGAGTCTGGAGGAGGGTGAG-TAMRA3'
per3	Forward	5'-AGCCAGTAACGACAAAGACATAG-3'
	Reverse	5'-CTCGAAGAGGTGATGCTGAC-3'
	Probe	5'FAM-ACAAACTTCTCTTGCAGCCGGTTCA-TAMRA3'
tnfa	Forward	5'-CCCTCCAGAAAAGACACCATG-3'
	Reverse	5'-GCCACAAGCAGGAATGAGAAG -3'
	Probe	5'FAM-CACAGAAAGCATGATCCGCGACG-TAMRA3'
il1b	Forward	5'-TCCTGTGTAATGAAAGACGGC-3'
	Reverse	5'-ACTCCACTTTGCTCTTGACTTC-3'
	Probe	5'FAM-TTGGGTATTGCTTGGGATCCACACTC-TAMRA3'
il18	Forward	5'-GCCTCAAACCTTCCAAATCAC-3'
	Reverse	5'-GTTGTCTGATTCCAGGTCTCC-3'
	Probe	5'FAM-TGCCATGTCAGAAGACTCTTGCGT-TAMRA3'

nlrp3	Forward	5’-ATGGGTTTGCTGGGATATCTC-3’
	Reverse	5’-GCGTTCCTGTCCTTGATAGAG-3’
	Probe	5’FAM-AGAACCTGCTTCTCACATGTCGTCTG-TAMRA3’
leptin	Forward	5’-AGCCTCACTCTACTCCACAG-3’
	Reverse	5’-CCTCTACATGATTCTTGGGAGC-3’
	Probe	5’FAM-TCAGCATTCAGGGCTAACATCCAACT-TAMRA3’
adipsin	Forward	5’-CCTGAACCCTACAAGCGATG-3’
	Reverse	5’-CAACGAGGCATTCTGGGATAG-3’
	Probe	5’FAM-CCGGGTGAGGCACTACACTCTG-TAMRA3’

3.4 FLOW CYTOMETRY

Table 3 shows the applied antibodies to analyze leukocyte subsets both in peripheral blood and digested tissues. Singlets were gated using FSC-A and FSC-H. Within singlets and the CD45+ gate, CD11b+Ly6G+ (neutrophils), CD11b+CD115+Ly6G- (monocytes and macrophages) and CD11b-Ly6G-SSClow (lymphocytes) populations were determined. Mean fluorescence intensity (geometric mean) of antibody-labeled adhesion molecules (CD11b CD49d, CD62L, CXCR4, and CD29) was measured. Cell counts were determined using CountBright™ Plus Absolute Counting Beads (Invitrogen, Cat. No.: C36995).

Table 3. Conjugated antibodies for flow cytometry measurement.

Mix IDs	Antibody	Conjugate	Clone	Cat. No.
Peripheral blood	CD45	FITC	30-F11	11-0451
	CD11b	eFluor450	M1/70	48-0112
	Ly6G	PE	1A8-Ly6g	12-9668
	CD115	APC	AFS98	17-1152
Leptin treatment 1	Ly6G	FITC	1A8-Ly6g	11-9668
	CD11b	eFluor450	M1/70	48-0112
	CD49d	PerCP-eFluor 710	R1-2	46-0492
	CD62L	PECy7	MEL-14	25-0621
	CXCR4	APC	L276F12	BZ-146507
Leptin treatment 2	Ly6G	PE	1A8-Ly6g	12-9668
	CD11b	eFluor450	M1/70	48-0112
	CD29	APC-eFluor 780	HMb1-1	47-0291

Digested tissue	CD45	PeCy7	30-F11	25-0451
	Ly6G	FITC	1A8-Ly6g	11-9668
	CD11b	eFluor450	M1/70	48-0112

3.5 PERIPHERAL BLOOD SAMPLING

Blood samples were collected at six different time points (ZT1, 5, 9, 13, 17, 21) from tail snip to determine absolute leukocyte counts of different cell subsets (Table 3) and to analyze adhesion molecule expression on the cell surface (Table 3, Peripheral blood). Serum samples were prepared from 0.8 ml blood collected through retroorbital bleeding.

3.6 EX VIVO LEPTIN TREATMENT OF WHITE BLOOD CELLS

40 µl of blood was collected from NC-AL-fed animals with a tail snip at ZT1. Samples were transferred into serum-free RPMI 1640 media supplemented with 50 U/ml penicillin and 50 µg/ml streptomycin and cells were incubated for 30 minutes at 37 °C in a 5% CO_2 atmosphere. Next, samples were treated with 15 ng/ml mouse leptin (Sigma, Cat. No.:GF050) or vehiculum for 4 h. After that, selectin and integrin subunits (CD62L, CD29, CD49d) and expression of the chemokine receptor CXCR4 were analyzed using flow cytometry (Table 3, Leptin treatment 1 and 2).

3.7 K/BXN SERUM-TRANSFER ARTHRITIS

K/BxN serum-transfer arthritis (STA) was induced by intraperitoneal injection of 250 µl arthritogenic serum (Day 0). Arthritis severity was assessed on day 6, corresponding to the peak of disease manifestation. Clinical scoring (1: no inflammation, 10: the worst condition according to (118)), ankle thickness measurements with a caliper (Koeplin), and functional, grid-holding ability tests (the duration of the upside-down grid holding was measured according to (118)) were performed. For further analysis, after termination of the animals, hind limbs were collected and minced.

3.8 CONTACT HYPERSENSITIVITY

3.8.1 Acute and subacute model

In the acute model, mice were sensitized with 100 µl 3% TNCB (2,4,6-trinitrochlorobenzene) solution applied on the shaved abdomen, whereas non-sensitized

animals were vehicle-treated with 100 µl of acetone on day 1. In the elicitation phase, ears of all animals were treated with 20 µl 1% TNCB solution on day 6. 24 hours later, contact hypersensitivity (CHS) severity was assessed. Ear thickness was measured using a caliper, and after termination of the animals, ears were minced for further analysis. All intervention was performed at ZT5.

To assess recovery capacity, ear thickness was monitored in two different models. The acute model was obtained after CHS induction, and TNCB-challenged ears were measured daily until day 20. Macroscopic images were taken on day 16. In addition, the subacute model was also conducted by applying TNCB challenges to the ears on three consecutive days in a row (days 6-8). Moreover, the development of ear swelling was measured daily until day 20. We repeated the subacute experiment with an experimental group fed AL before disease induction and transitioned to TRF after the first TNCB treatment. Similarly to the acute model, after termination of the animals, macroscopic images were captured on day 16 as well.

3.8.2 Administration of leptin receptor antagonist

Ears of the HF-AL or *db/db* sensitized animals were treated with intradermal injection of leptin receptor antagonist, Allo-aca (MCE®, Cat. No.: HY-P3212, 10 ng/g body weight) or with vehicle on day 6 at ZT1. At ZT5, both ears were TNCB challenged. 24 hours later, the impact of Allo-aca treatment was assessed as described in the previous section.

3.9 ENZYMATIC DIGESTION OF EAR- AND ANKLE TISSUE SAMPLES

Tissue samples were digested in HBSS (Gibco, Cat. No.: 14025092) containing 200 µg/ml liberase TM (Roche, LIBTM-RO, Cat. No.: 5401127001), 1 µg/mL DNase I (Roche, Cat. No.: 10104159001), and 200 mM HEPES (pH=7.4, Gibco, Cat. No.: 15630080). Ankle samples were incubated in 1 ml digesting solution at 37 °C for 1 hour on a horizontal shaker (1400 rpm). Ear samples were digested in 500 µl solution at 37 °C for 45 min, 1200 rpm. Samples were flushed with 2 × 500 µl PBS through a 70 µm stainer. After centrifugation (5 minutes at 1000 g, 4 °C), the supernatant was collected for measurement of protein levels, and the pellet was resuspended in PBS (with 5% FBS) for flow cytometric analysis (Table 3, digested tissue).

3.10 QUANTIFICATION OF CYTOKINE AND HORMONE LEVELS IN SERUM AND TISSUE SAMPLES

Concentrations of corticosterone, leptin, IL-1ß, and CXCL2 were determined from serum and supernatants of tissue lysates using R&D systems ELISAs (Cat. No.: KGE009, MOB00B, MLB00C-1, and MM200) according to the manufacturer's instructions.

3.11 STATISTICAL ANALYSIS

Paired t-tests and two-sample t-tests were performed in Excel 2016. One-way and two-way ANOVAs were conducted in Statistica software (version 14.0.1, StatSoft), followed by either Fisher LSD or Tukey HSD (Unequal N) post-hoc tests, as appropriate. Cosinor analysis was carried out in Matlab R2021a (MathWorks), with p-values indicating the statistical significance of the fitted curves ($p>0.05$ indicates a dampened rhythm; $p<0.05$ indicates a robust rhythm). Statistical significance was defined as $p<0.05$.

4. RESULTS

4.1 METABOLIC EFFECTS OF HIGH-FAT DIET AND TIMED FOOD INTAKE

4.1.1 Metabolic parameters under different feeding conditions

Caloric intake and weight gain were monitored throughout the 4-week conditioning. Weekly caloric intake in the HF groups was significantly higher than that in the NC groups (Figure 8A). Interestingly, TRF did not result in a reduction of the caloric intake when compared to the corresponding *ad libitum* group. However, weight gain showed more pronounced elevation in AL-fed animals (Figure 8B). In line with previous observations of Hatori et al. (28), HF-AL had significantly more daytime caloric intake than NC-AL (Figure 8C). Although fasting glucose levels were slightly elevated in the HF groups compared to NC-fed groups (Figure 8D), in the intraperitoneal glucose tolerance test (IPGTT), blood glucose levels and the area under the curve (AUC) did not significantly differ across the experimental groups (Figure 8E). Thus, a short-term HF diet had minimal effect on the glucose homeostasis of the animals.

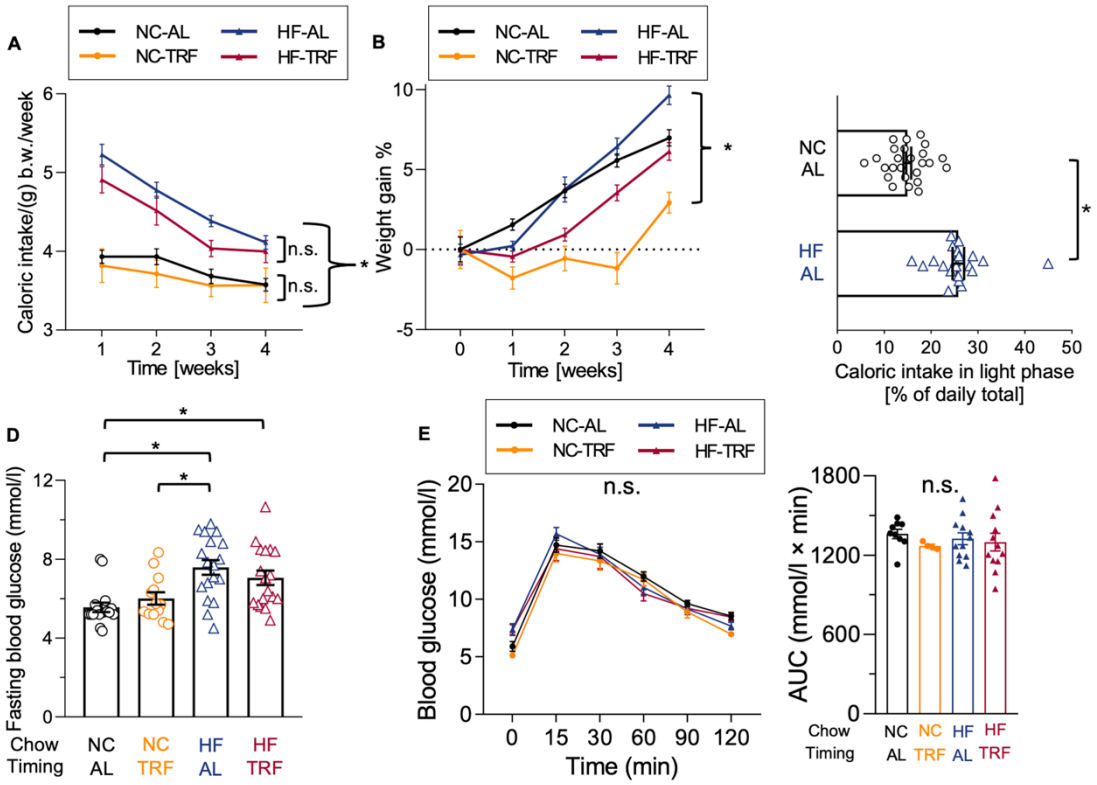

*Figure 8. Metabolic parameters of the experimental groups. (A) Caloric intake during the 4-week conditioning to different feeding programs. Weekly recorded food consumption was normalized to g body weight. Mean ± SEM, n(NC-AL)cages=23, n(NC-TRF)cages=7, n(HF-AL)cages=20, n(HF-TRF)cages=24. Repeated Measures ANOVA, *p<0.05, significant group and group x time effect. (B) Body weight gain of the experimental groups during the 4-week conditioning. Weekly measured body weight was normalized to values obtained right before the beginning of the 4-week feeding schedule. Mean ± SEM, n(NC-AL)=132, n(NC-TRF)=37, n(HF-AL)=139, n(HF-TRF)=128. Repeated Measures ANOVA, *p<0.05, significant group and group x time effect. (C) Caloric intake in the light period of the day was measured on each day and averaged for the 4-week period. Mean ± SEM, n(NC-AL)=25, n(HF-AL)=21, two sample t-test, *p<0.05. (D) Fasting blood glucose levels. Mean ± SEM, n(NC-AL)=17, n(NC-TRF)=13, n(HF-AL)=18, n(HF-TRF)=18. One-way ANOVA, Post Hoc Tukey's HSD unequal N test, *p<0.05, significant group effect. (E) Time restricted-feeding and high-fat diet have no impact on intraperitoneal glucose tolerance test. Left panel: Intraperitoneal Glucose Tolerance Test (IPGTT). Mean ± SEM, n(NC-AL)=9, n(NC-TRF)=4, n(HF-AL)=12, n(HF-TRF)=12. Repeated Measures ANOVA, *p<0.05, no significant group effect. Right panel: The area under the curve (AUC) was calculated for the IPGTT measurements. Mean ± SEM, n(NC-AL)=9, n(NC-TRF)=4, n(HF-AL)=12, n(HF-TRF)=12, One-way ANOVA, *p<0.05, no significant (n.s.) group effect.*

Serum corticosterone levels were measured at six time points to assess the circadian operation and stress levels of the animals (Figure 9). In the NC-TRF and HF groups the daily average of corticosterone concentrations was slightly elevated (Figure 9); however, hormone levels remained below the stress threshold, which is typically considered to be

around 300-500 ng/mL (119, 120). In NC-fed groups, the acrophase of the rhythm occurred at approximately ZT14 (Table 4). Hence, a phase difference was detected when compared to ZT9 in HF-AL and to ZT6 in HF-TRF animals, indicating that HF diet influences circadian operation.

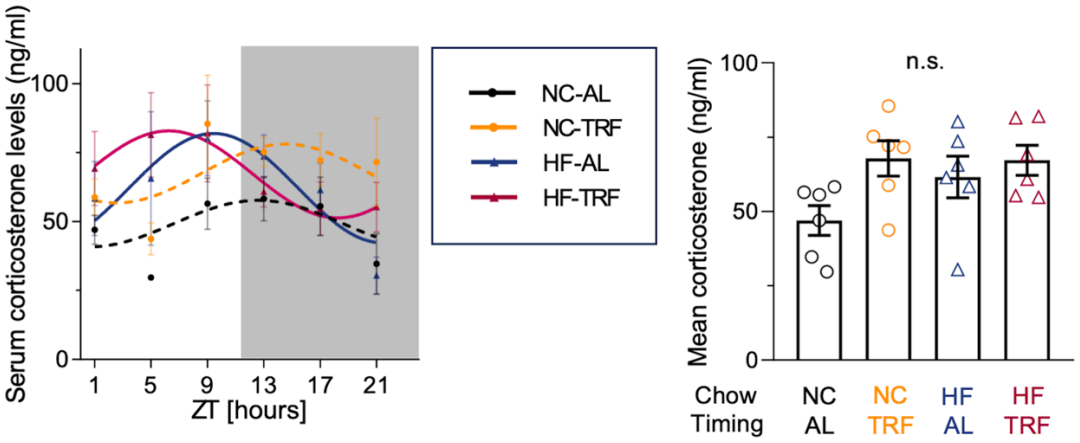

Figure 9. Assessing circadian clock-regulated corticosterone levels. Left panel: Serum corticosterone rhythms in the experimental groups. Mean ± SEM, n/time point (NC-AL)=3-11, n/time point (NC-TRF)=3-11, n/time point (HF-AL)=3-5, n/time point (HF-TRF)=3-5. Solid lines indicate significant ($p<0.05$), whereas dashed lines indicate non-significant cosine curve fit. Right panel: Mean corticosterone levels in the experimental groups. Daily means were calculated using data shown in the left panel. Mean ± SEM, n=6, one-way ANOVA, n.s not significant. ZT=Zeitgeber time

Table 4. Cosinor analysis of serum corticosterone levels. P-values indicate the statistical significance of fitted curves.

		NC-AL	NC-TRF	HF-AL	HF-TRF
Serum Corticosterone	Amplitude	11.77	13.21	20.1	15.7
	Acrophase (ZT)	13.38	14.24	9.6	6.31
	Mesor	46.93	67.85	61.62	67.25
	p-value	0.1287	0.182	0.0152	0.0002

4.1.2 Circadian gene expression profile of the white adipose tissue depends on both timing and composition of the diet

Epididymal visceral white adipose tissue (WAT) was collected after 4 weeks of conditioning at six timepoints. My collegues showed that the core clock component *per2* has elevated amplitude in its daily levels in NC-TRF compared to that of NC-AL mice. Additionally, *reverbα*, an element of the stabilizator loop, and known to be sensitive to metabolic changes, showed a phase shift in NC-TRF, confirming that TRF influences the

clock in WAT (66). This effect on WAT clock in NC-TRF resulted in strengthened rhythmicity and a decrease in the production of the inflammatory adipokine leptin (66). Therefore, gene expression of other *CCGs* was also analyzed. NC-TRF significantly decreased daily average expressions of *tnfa, adipsin, nlrp3, il18,* but not *il-1ß*, compared to NC-AL (Figure 10). Overall, TRF entrained the clock of WAT, decreased gene expression of inflammatory mediators and inflammasome pathway components.

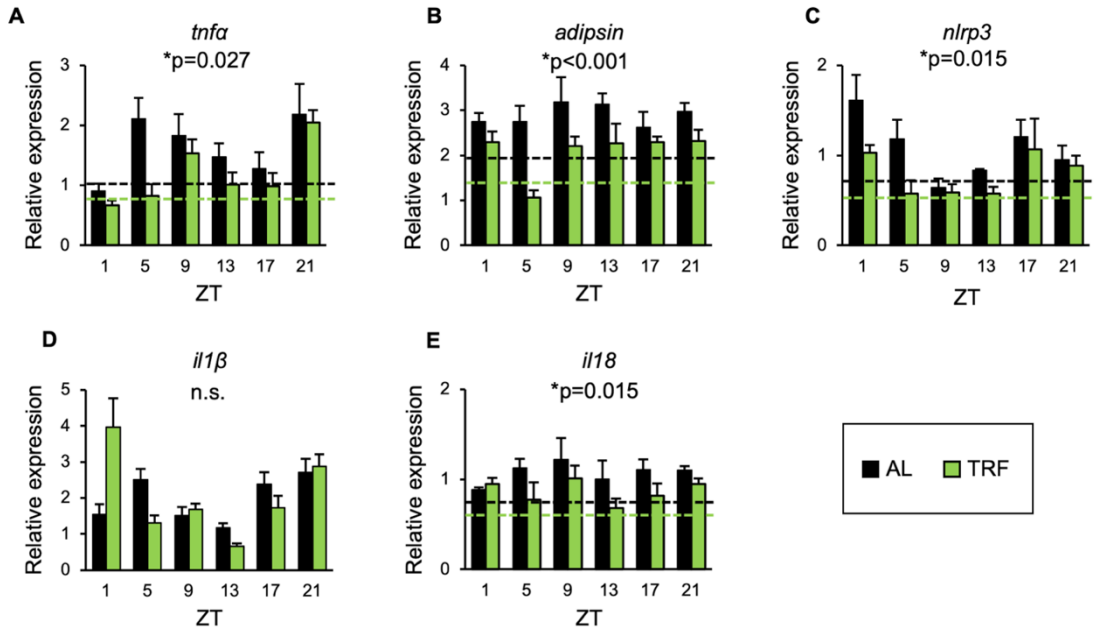

*Figure 10. Time-restricted feeding reduces gene expression of inflammatory mediators in visceral adipose tissue. Relative mRNA expression of (A) tnfα, (B) adipsin, (C) nlrp3, (D) il-1ß and (E) il-18 in the course of day in WAT. Mean + SEM, n/time point (NC-AL)=3-9, n/time point (NC-TRF) =6-11, two-way ANOVA, p<0.05, * indicates significant group effect. Rplp0 was used as a reference gene. Dashed lines indicate average daily mRNA expression of the indicated gene, where a significant group effect persists. ns, not significant. ZT=Zeitgeber time*

To address the effect of the high-fat diet on the WAT clock, negative factors of the core loop, *per1, per3,* and a component of the secondary loop, *dbp,* were measured in both NC and HF groups. Interestingly, NC-TRF dampened both the expression and the amplitude of the clock genes *per1, per3,* and *dbp* compared to NC-AL, albeit maintaining the rhythmic manner of their expression (Figure 11, Table 5). My colleagues observed a similar effect of TRF on clock genes expression in brown adipose tissue (data not shown); however, further investigation is still needed. In HF-AL mice, a dampened and phase-advanced rhythm of the *per1* and *per3* clock genes was detected in WAT compared to the NC-AL fed group, whereas the rhythmicity of *dbp* was not affected. According to the

cosinor analysis, HF-TRF rescued these effects on *per1* and *per3* expression (Figure 11, Table 5). In summary, HF diet dampened the clock operation of WAT hence, TRF ameliorated this effect, which may contribute to the beneficial metabolic effects of timed food intake.

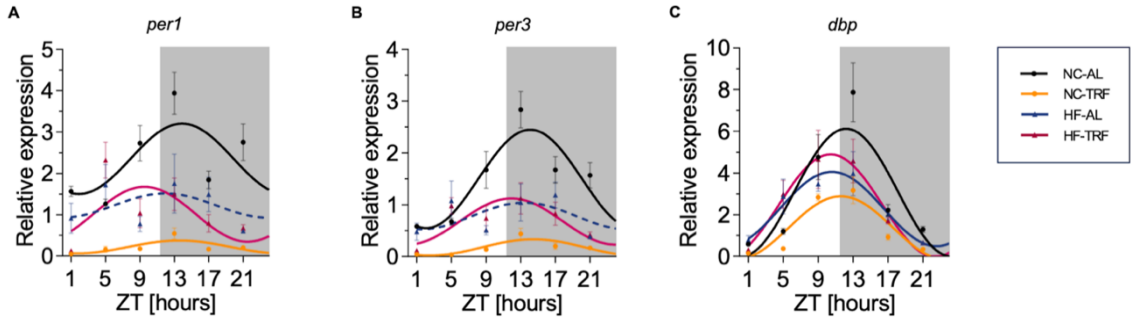

Figure 11. High-fat diet dampens the operation of the peripheral clock in white adipose tissue. Cosine curve fit to relative mRNA expression of (A) per1, (B) per3, and (C) dbp. Mean ± SEM, n/time point (NC-AL)=7-9, n/time point (NC-TRF)=6-11, n/time point (HF-AL)=4-7, n/time point (HF-TRF)=5-7. Solid lines indicate significant, fixed 24-hour period cosine curve fit with cosinor analysis, whereas dashed lines show non-significant fit. ZT=Zeitgeber Time

Table 5. Cosinor analysis of the expression of clock genes in white adipose tissue. P values indicate the statistical significance of fitted curves.

Clock gene	Circadian parameter	Group			
		NC-AL	NC-TRF	HF-AL	HF-TRF
per1	Amplitude	0.8047	0.1533	0.2809	0.5899
	Acrophase (ZT)	13.9563	13.5941	11.9003	8.7245
	Mesor	2.3161	0.2204	1.2289	1.0851
	p value	0.0043	0.0041	0.5366	0.0184
per3	Amplitude	0.9474	0.1615	0.2373	0.4025
	Acrophase (ZT)	14.0955	14.4541	13.4509	11.7803
	Mesor	1.4999	0.1749	0.7954	0.7007
	p value	0.0000	0.0001	0.2766	0.0064
dbp	Amplitude	3.2201	1.5725	1.7597	2.4118
	Acrophase (ZT)	12.2566	11.6892	10.5327	10.3620
	Mesor	2.9829	1.3424	2.2863	2.4633
	p value	0.0000	0.0000	0.0000	0.0000

Leptin is clock-controlled in the WAT (49). To follow the consequences of the diets on the rhythmic function of WAT, leptin expression was investigated. NC datasets were taken from Ella et al (66). HF-AL increased *leptin* expression and phase-advanced its rhythm (Figure 12A, Table 6). However, in HF-TRF mice, leptin expression was

significantly lower compared to the AL-fed animals and peaked at night, which suggests a compensatory effect of timed eating.

Serum leptin levels were also measured at six timepoints (Figure 12B, Table 6). Parallel with gene expression, NC-AL samples showed no significant rhythm, while in the NC-TRF group lowered serum leptin levels with robust rhythmicity were detected. The HF-AL group had significantly elevated and phase shifted leptin levels compared to the NC groups, whereas HF-TRF prevented this negative effect and stabilized the rhythmicity. Besides being a *ccg,* leptin is an important adipokine. It acts via cytokine receptors, positioning it as a potential link between metabolic regulation and immune responses; hence, this interaction may be modulated by time-restricted feeding.

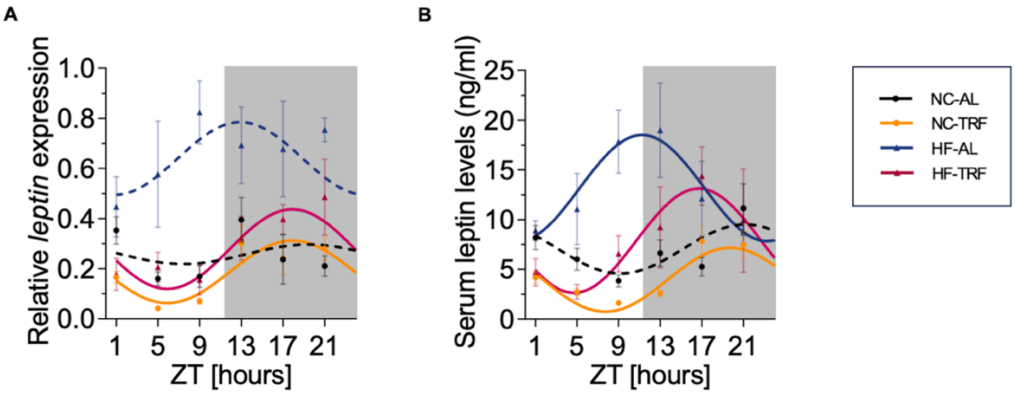

Figure 12. Relative mRNA expression of leptin in white adipose tissue and corresponding serum leptin levels throughout the day. Mean ± SEM, (A) Time-of-the-day-dependent changes in relative leptin expression. n/time point (NC-AL)=7-9, n/time point (NC-TRF)=6-11, n/time point (HF-AL)=4-7, n/time point (HF-TRF)=5-7. (B) Serum leptin levels in the course of the day. n/time point(NC-AL)=3-7, n/time point(NC-TRF)=3-8, n/time point(HF-AL)=3-5, n/time point(HF-TRF)=3. Solid lines indicate significant, fixed 24-hour period cosine curve fit with cosinor analysis, whereas dashed lines show non-significant fit.

Table 6. Cosinor analysis of relative leptin expression and serum leptin levels. P-values indicate the statistical significance of fitted curves.

		NC-AL	NC-TRF	HF-AL	HF-TRF
Relative *leptin* expression	Amplitude	0.0396	0.125	0.111	0.175
	Acrophase (ZT)	16.97	17.66	13.30	16.99
	Mesor	0.254	2.800	0.661	0.278
	p-value	0.7714	0.0182	0.2642	0.0220
Serum leptin levels	Amplitude	2.66	3.21	5.59	5.20
	Acrophase (ZT)	21.96	19.78	11.35	16.75
	Mesor	6.85	4.40	12.92	7.91
	p-value	0.0729	0.0039	0.0008	0.0009

4.2. EFFECTS OF TIMED FOOD INTAKE ON IMMUNE RESPONSIVENESS

4.2.1 Expression of adhesion molecules on myeloid cells under steady-state conditions

Ella et al. demonstrated that TRF enhances the amplitude of leukocyte count rhythm in peripheral blood (66). As the acrophase of leukocyte count is at ZT5, cell subpopulations were investigated at this time point after HF conditioning as well. However, total white blood cells and leukocyte subpopulations, neutrophils and monocytes, showed no alterations after 4-week conditioning (Figure 13A-C).

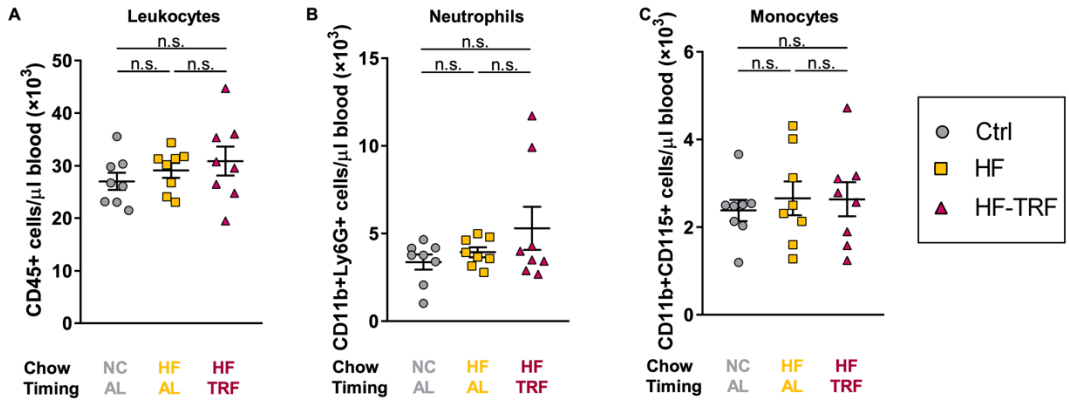

*Figure 13. Analysis of blood leukocyte subsets. (A) Leukocyte (CD45+), (B) neutrophil (CD45+, Ly6G+), and (C) monocyte (CD45+, CD11b+,CD115+) counts in blood at ZT5 in steady-state. Mean ± SEM, n=8 / group, One-way ANOVA, *p<0.05, n.s.: not significant.*

Zarkesh-Esfahani and colleagues demonstrated that leptin can indirectly increase CD11b expression in human neutrophils (104). Further studies are underway to determine whether CD11b expression correlates with diet-induced changes in leptin levels. HF diet triggers the elevation of serum leptin, which can be prevented by TRF. Expression of the activation marker CD11b, was determined on neutrophils and monocytes at six time points after the 4-week conditioning (Figure 14A, B). In the HF-AL group, the daily average of CD11b expression was increased on neutrophils, which was prevented by TRF. Similarly, HF-AL significantly elevates CD11b on the surface of the monocyte population and TRF prohibited this effect. These data support the idea that even a short-term HF diet promotes priming and facilitates migration of myeloid cells, whilst TRF has a preventive effect.

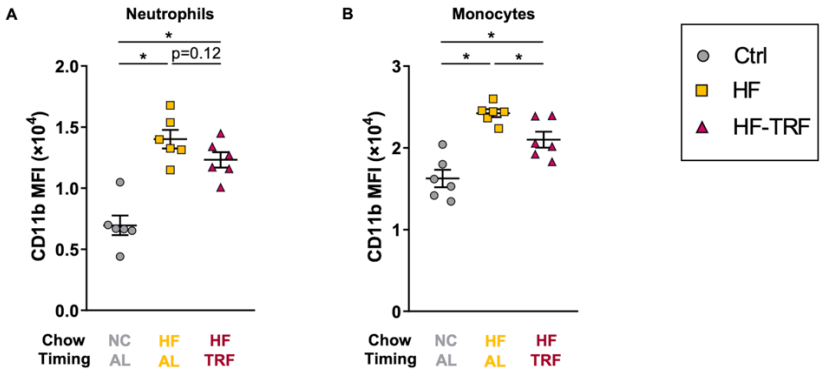

*Figure 14. Daily average CD11b expression on circulating (A) neutrophils and (B) monocytes in steady-state. Blood samples of animals subjected to the feeding schedules for 4 weeks were collected at six designated time points (ZT1, 5, 9, 13, 17, 21) and subsequently analyzed. The daily average CD11b level was calculated in each group. n=3/time point/group, Mean ± SEM, One-way ANOVA, Post Hoc Fisher LSD Test, *p<0.05, MFI: mean fluorescent intensity.*

4.2.2 *Ex vivo* leptin stimulation of isolated peripheral blood leukocytes

Our research group found that NC-TRF decreases the MFI levels of CD62L, CD29, CD49d, and CXCR4 on the surface of neutrophils and monocytes compared to the NC-AL fed group after a 4-week conditioning period (66). To address leptin's role in adhesion molecule expression, blood of NC-AL-fed mice was collected at ZT1 and treated with 15 ng/ml leptin for 4 hours. Leptin treatment tendentiously elevated the expression of CD62L and CD29. CD49d on both myeloid cell types and CXCR4 on monocytes were significantly increased compared to vehicle treatment (Figure 15), which suggests that leptin may contribute to the elevated migratory capacity of neutrophils and monocytes.

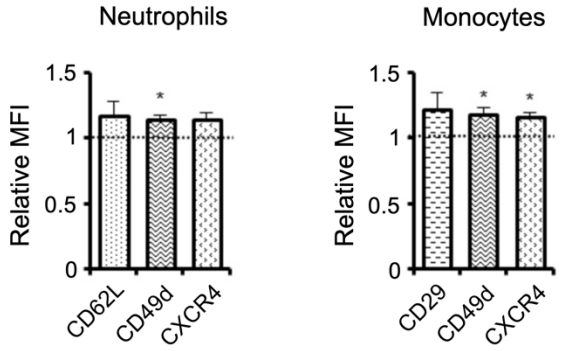

*Figure 15. Expression of migratory factors of neutrophils and monocytes after leptin treatment. CD62L selectin, integrin subunits (CD29, CD49d), and chemokine receptor (CXCR4) expression of (A) neutrophils and (B) monocytes after 4-hour leptin treatment compared to vehicle. Mean + SEM, n=5, one-sample t-test, *p<0.05.*

In conclusion, leptin treatment directly elevated the expression of adhesion molecules and the CXCR4 receptor. Emerging evidence suggests that a high-fat diet contributes to the priming of myeloid cells, a process that is at least partially mediated by leptin. Since these cells play a critical role in the development of autoimmune responses, and TRF has a leptin-lowering effect, our subsequent investigations aimed to explore how timed food intake influences the progression of an autoimmune disease.

4.3 TRF IMPROVES INFLAMMATION OUTCOMES

4.3.1 Effect of TRF and HF diet on the development of K/BxN serum transfer arthritis

We demonstrated that NC-TRF alleviated symptoms of STA compared to NC-AL-fed animals (66). We also showed that this is partially due to a significant decrease in the number of neutrophils in the synovium (Figure 16).

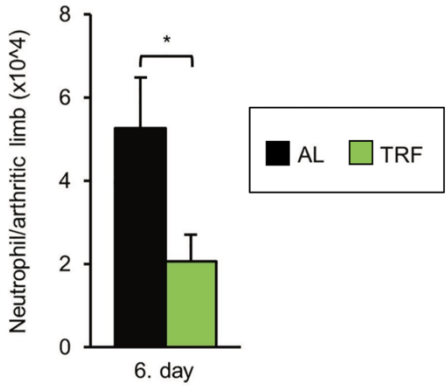

*Figure 16 Neutrophil counts in the arthritic hind limbs of NC-fed mice. Mean+SEM, n=7 (AL), n=7 (TRF), two-sample t-test, * $p < 0.05$).*

To investigate how HF diet affects arthritis severity, STA was induced in Ctrl (NC-AL), HF-AL and HF-TRF groups. To eliminate body weight as a confounding factor in arthritis severity, animals were selected to have similar weights, which was confirmed by measurements taken prior to inflammation induction (Figure 17).

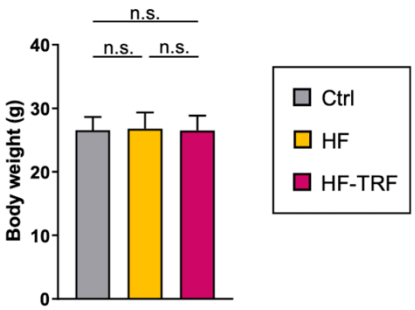

Figure 17. Body weight of the animals subjected to STA after 4-week conditioning. n(Ctrl/NC-AL)=17, n(HF)=16, n(HF-TRF)=17, Mean + SD, One-way ANOVA, n.s. not significant.

At the peak of the arthritis symptoms (day 6), disease severity was assessed using clinical scoring and ankle thickness measurement (Figure 18A, B). In addition, a functional grid-holding ability test was performed (Figure 18C). There were no differences in the phenotype between HF-AL and Ctrl (NC-AL) mice, whereas HF-TRF reduced all parameters below NC-AL and HF-AL values.

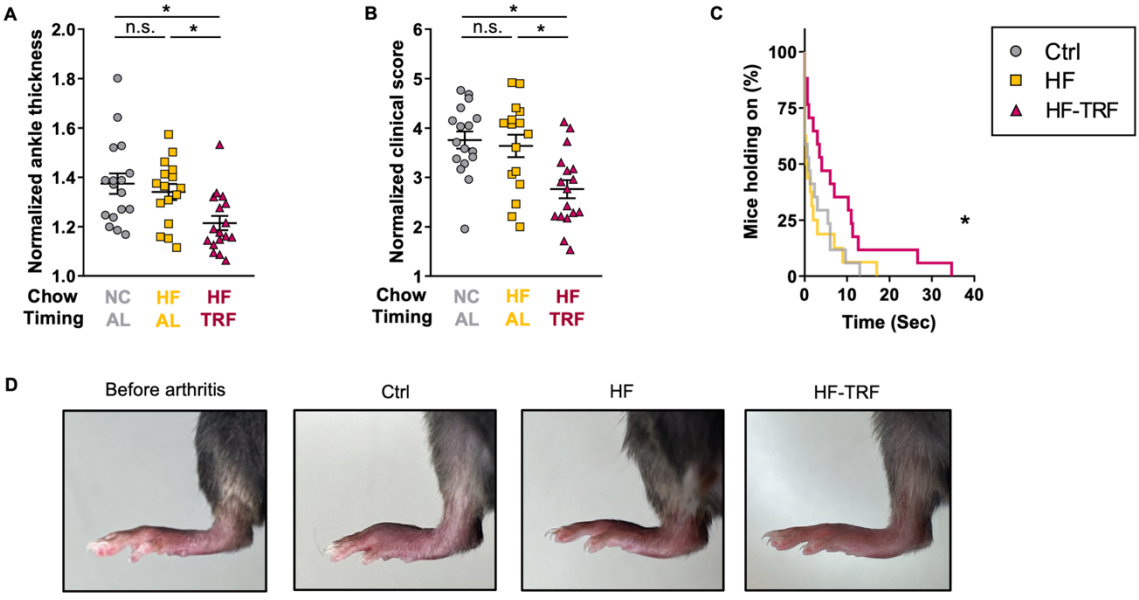

*Figure 18. Macroscopic analysis of STA. Ankle thickness of (A) the limbs and (B) clinical scoring were normalized to values measured directly before arthritis induction (day 0). n(Ctrl/NC-AL)=17, n(HF)=16, n(HF-TRF)=17, Mean ± SEM, One-way ANOVA, Post Hoc Fisher LSD Test, *p<0.05, n.s., not significant. (C) Grid-holding ability of the animals. n(Ctrl)=17, n(HF)=16, n(HF-TRF)=17, Log-rank (Mantel-Cox) test, curve comparison, *p<0.05. (D) Representative pictures of the hind limbs.*

According to flow cytometry analysis of the digested limbs, HF-AL feeding slightly increased leukocyte counts and significantly elevated the counts of infiltrated neutrophils compared to the Ctrl (NC-AL) (Figure 19A, B, C). This finding indicates that neutrophils

could be the main contributors to the inflammation-worsening effect mediated by HF diet. However, in HF-TRF mice, significantly decreased synovial leukocyte count, myeloid leukocyte count, and leptin and IL-1ß levels (Figure 19B-E) were detected. These data suggest that anti-inflammatory mechanism of TRF may partially be mediated through leptin reduction. Although the STA model provides valuable insights, it has certain limitations. Notably, arthritis severity is influenced by body mass, and the model only allows investigation of the effector phase of the disease. These limitations underscore the need for further studies exploring other inflammatory disease models to gain a more comprehensive understanding of how TRF affects immune responsiveness.

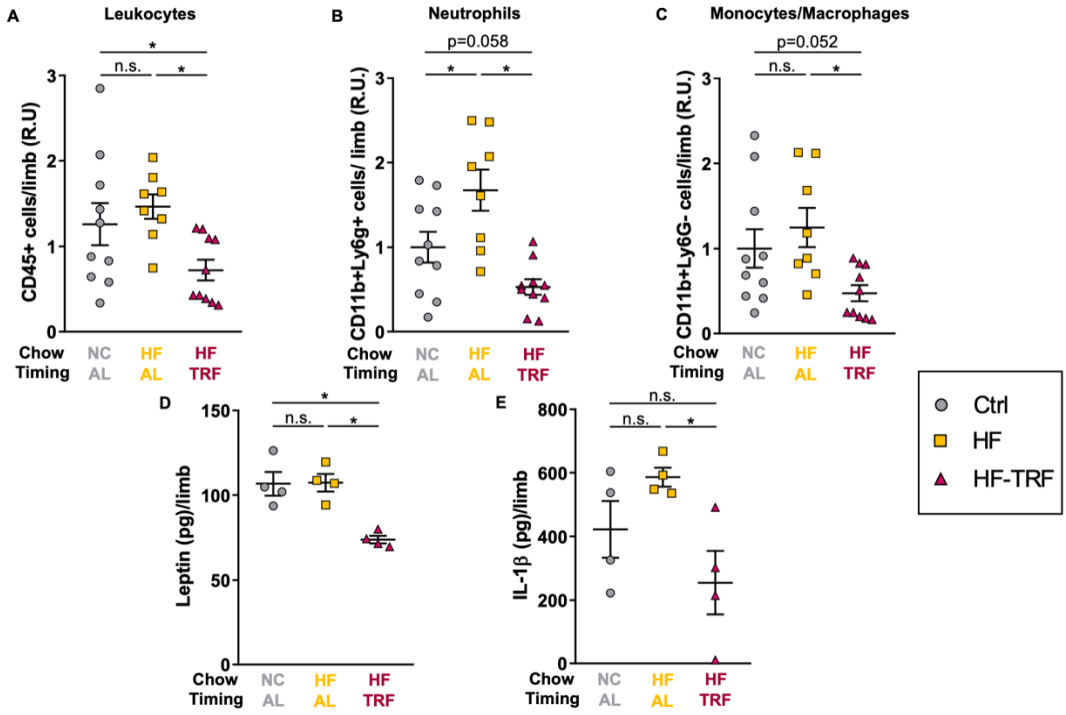

*Figure 19. Analysis of leukocytes and cytokines in arthritic limbs, and of steady-state blood leukocyte subsets. (A) Leukocyte (CD45+), (B) neutrophil (CD45+, CD11b+, Ly6G+), and (C) monocyte/macrophage (CD45+, CD11b+, Ly6G-) counts in the digested limb samples at ZT5. In distinct experiments, values were normalized to average cell counts measured in the control samples. n(Ctrl)=10, n(HF)=8, n(HF-TRF)=10, Mean ± SEM, One-way ANOVA, Post Hoc Fisher LSD Test, *p<0.05, n.s.: not significant. R.U. relative unit. (D) Synovial leptin and (E) IL-1β levels. n=4/group, Mean ± SEM, One-way ANOVA, Post Hoc Fisher LSD Test, *p<0.05, n.s.: not significant.*

4.3.2 Investigation of diets' effects on acute and subacute contact hypersensitivity

TNCB-induced contact hypersensitivity (CHS), the mouse model of human allergic contact dermatitis (ACD), was performed. CHS severity was assessed 24 hours post-challenge in both non-sensitized and sensitized mice (Figure 20A, Figure 21A). Interestingly, HF animals subjected to TNCB challenge without sensitization also significantly increased ear swelling, IL-1ß, and neutrophil count compared to all other experimental groups (Figure 20B-D). These parameters were, however, compensated by TRF.

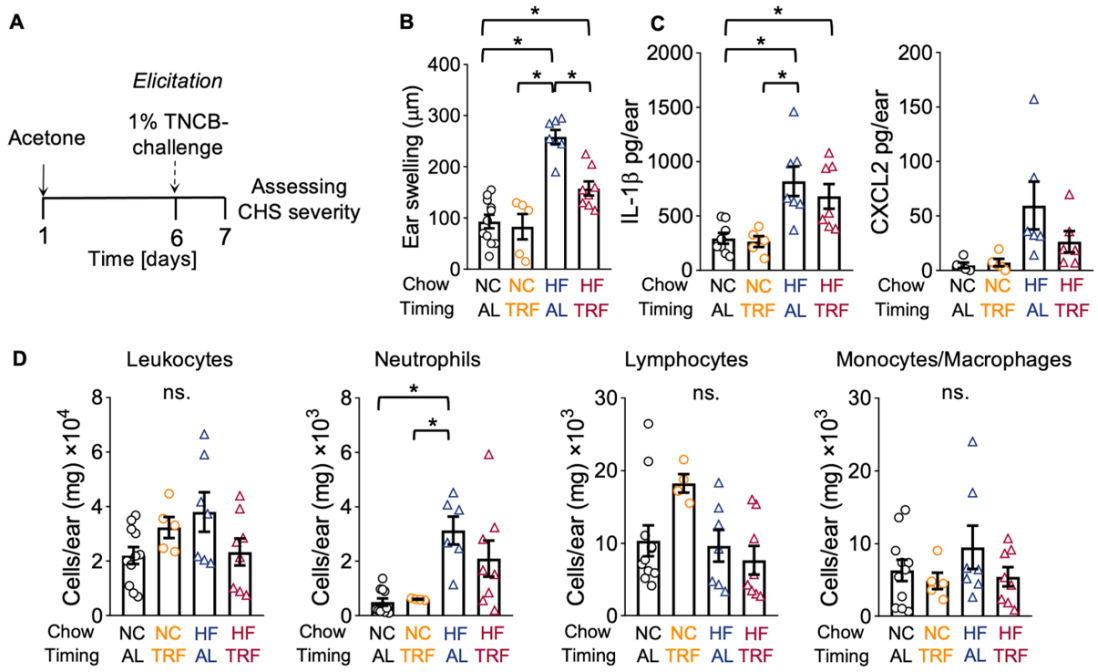

*Figure 20. Assessing CHS severity in non-sensitized mice. (A) Experimental design of TNCB-induced CHS. After four weeks of conditioning, non-sensitized animals received acetone on the shaved abdomen. Five days later, ears were challenged using 1% TNCB solution. Inflammation severity was assessed 24 hours later, on day 7. (B) Ear swelling depends on the timing and content of the diet. Ear thickness measured on day 7 was normalized to that of measured on day 6 in the same animal. Mean ± SEM, n(NC-AL)=11, n(NC-TRF)=5, n(HF-AL)=7, n(HF-TRF)=8. One-way ANOVA, Post Hoc Tukey's HSD unequal N test, *p<0.05, significant group effect. (C) IL-1β and CXCL2 levels in ear lysates are diet-dependent. IL-1β: n(NC-AL)=8, n(NC-TRF)=5, n(HF-AL)=7, n(HF-TRF)=7. CXCL2: n(NC-AL)=5, n(NC-TRF)= 5, n(HF-AL)=6, n(HF-TRF)=6,. Mean ± SEM, One-way ANOVA, Post Hoc Tukey's HSD unequal N test, *p<0.05, significant group effect. (D) Accumulation of immune cells in ear lysates of the experimental groups. Indicated cell counts were determined by flow cytometry. Mean ± SEM, n(NC-AL)=11, n(NC-TRF)=4-5, n(HF-AL)=6-7, n(HF-TRF)=8. One-way ANOVA, Post Hoc Tukey's HSD unequal N test, *p<0.05, Leukocytes, lymphocytes, and monocytes/macrophages: no significant (ns.) differences, neutrophils: significant group effect.*

As expected, sensitization increased ear thickness compared to non-sensitized groups (Figure 20B, Figure 21B). The largest normalized ear thickness was detected in the sensitized HF-AL group, notably, HF-TRF prevented the ear thickening effect. Intriguingly, NC-TRF showed no beneficial effect compared to NC-AL. IL-1ß and CXCL2 levels, key mediators of the CHS model, were determined in ear lysates (Figure 21C). Next, infiltrated leukocytes were measured by flow cytometry. In sensitized HF groups, elevated leukocyte count was detected in the inflamed tissue (Figure 21D). Subset analysis showed that the monocyte/macrophage population did not differ between the groups, and lymphocyte counts showed no correlation with CHS severity. In contrast, association could be detected between neutrophil counts and CHS severity both in sensitized and non-sensitized groups (Figure 20D, Figure 21D). In addition, the highest neutrophil counts were detected in the tissues of sensitized HF-AL animals, an effect that was mitigated by the HF-TRF diet. These findings are further supported by the work of a student (Bernadett Vendl) under my supervision, who prepared ear tissue sections and applied hematoxylin and eosin (H&E) staining as well as anti-Gr-1 immunohistochemistry (data not shown). These analyses clearly demonstrated that HF treatment markedly enhanced the formation of intraepidermal pustules, which were densely infiltrated by neutrophils.

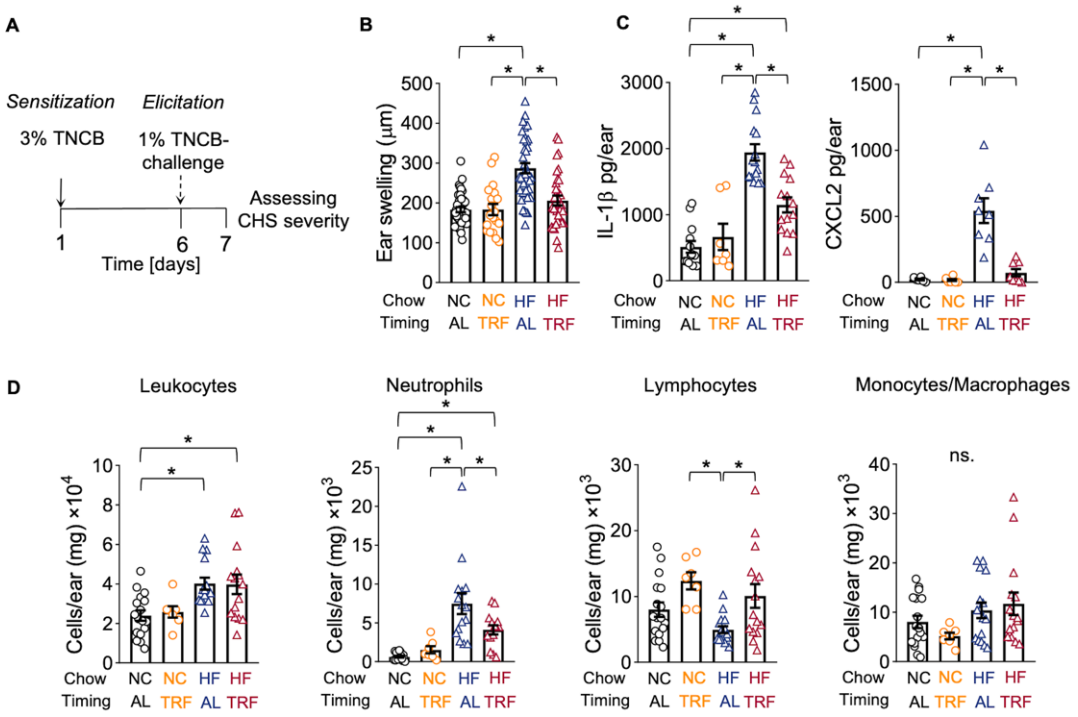

*Figure 21. Time-restricted feeding and high-fat diet affect the severity of symptoms of CHS. (A) Experimental design of TNCB-induced CHS. After four weeks of conditioning in the sensitization phase, the abdominal skin of mice was treated with 3 % TNCB. The elicitation phase was provoked using 1% TNCB solution applied to the ears on day 6. CHS severity was assessed 24 hours later, on day 7. (B) Ear swelling depends on the timing and content of the diet. Ear thickness measured on day 7 was normalized to that measured on day 6 in the same animal. Mean ± SEM, n(NC-AL)=40, n(NC-TRF)=19, n(HF-AL)=39, n(HF-TRF)=33. One-way ANOVA, Post Hoc Tukey's HSD unequal N test, *p<0.05, significant group effect. (C) IL-1β and CXCL2 levels in ear lysates are dependent on diet. IL-1β: n(NC-AL)=13, n(NC-TRF)=7, n(HF-AL)=15, n(HF-TRF)=16. CXCL2: n(NC-AL)=6, n(NC-TRF)=6, n(HF-AL)=8, n(HF-TRF)=7. Mean ± SEM, One-way ANOVA, Post Hoc Tukey's HSD unequal N test, *p<0.05, significant group effect. (D) Accumulation of immune cells in ear lysates of the experimental groups. Indicated cell counts were determined by flow cytometry. Mean ± SEM, n(NC-AL)=16-17, n(NC-TRF)=7, n(HF-AL)=15-16, n(HF-TRF)=14-15. One-way ANOVA, Post Hoc Tukey's HSD unequal N test, *p<0.05, Leukocytes, neutrophils, and lymphocytes: significant group effect, monocytes/macrophages: no significant (ns.) differences.*

To address the recovery of the experimental groups, regeneration kinetics of the acute and subacute models were investigated, similarly to the DNFB model (97). In the acute model, animals were sensitized and TNCB-challenged, then the regeneration of ears was investigated by daily ear thickness measurement during a two-week post-challenge period (Figure 22). Regeneration capacity of NC-AL, NC-TRF, and HF-TRF showed similar kinetics. The regeneration of HF-AL mice was, however, prolonged and no recovery

occurred during the observation period. Macroscopic images were taken on day 16, and scabs at the edge of the ear appeared only in the HF-AL group.

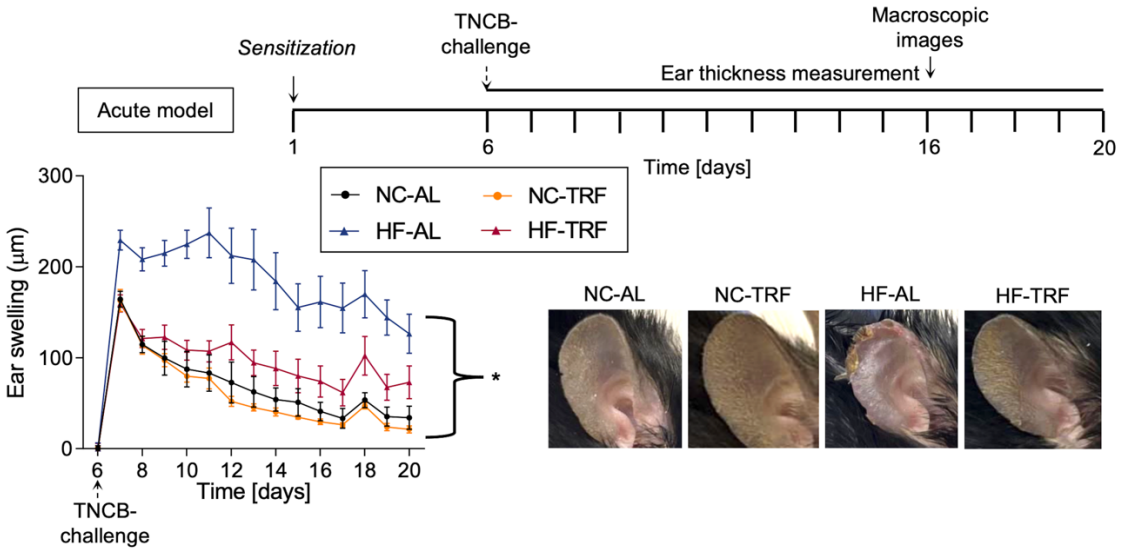

*Figure 22. Investigation of recovery in the acute model of CHS. Upper panel: schematic outline of the experiment. Left lower panel: Ear thickness normalized to data obtained on day 6. Mean ± SEM, n(NC-AL)=8-11, n(NC-TRF)=6-9, n(HF-AL)=9-12, n(HF-TRF)=9-12. Repeated measures ANOVA, significant group and group x time effect, *p<0.05. Right lower panel: Representative macroscopic images of the ears from the indicated groups, taken 10 days after the TNCB challenge.*

In the subacute model, TNCB-challenge was repeated on 3 consecutive days, then ear regeneration was detected, as in the acute model (Figure 23A). TRF significantly shortened the regeneration period even in mice fed with normal chow (Figure 23B). HF-AL feeding not only disrupted recovery but also exacerbated CHS severity, as evidenced by increased ear thickness measurements (Figure 23C). Consistent with these findings, scab size was increased in the HF-AL group, whereas only minor alterations were observed in the ear images of the HF-TRF groups (Figure 23C). To assess the therapeutic potential of TRF, a group of mice subjected to AL feeding was switched to TRF on day 7. Under both NC and HF conditions, the AL-TRF transition resulted in reduced ear swelling, indicating that TRF has beneficial effects even when applied after disease development (Figure 23B, C).

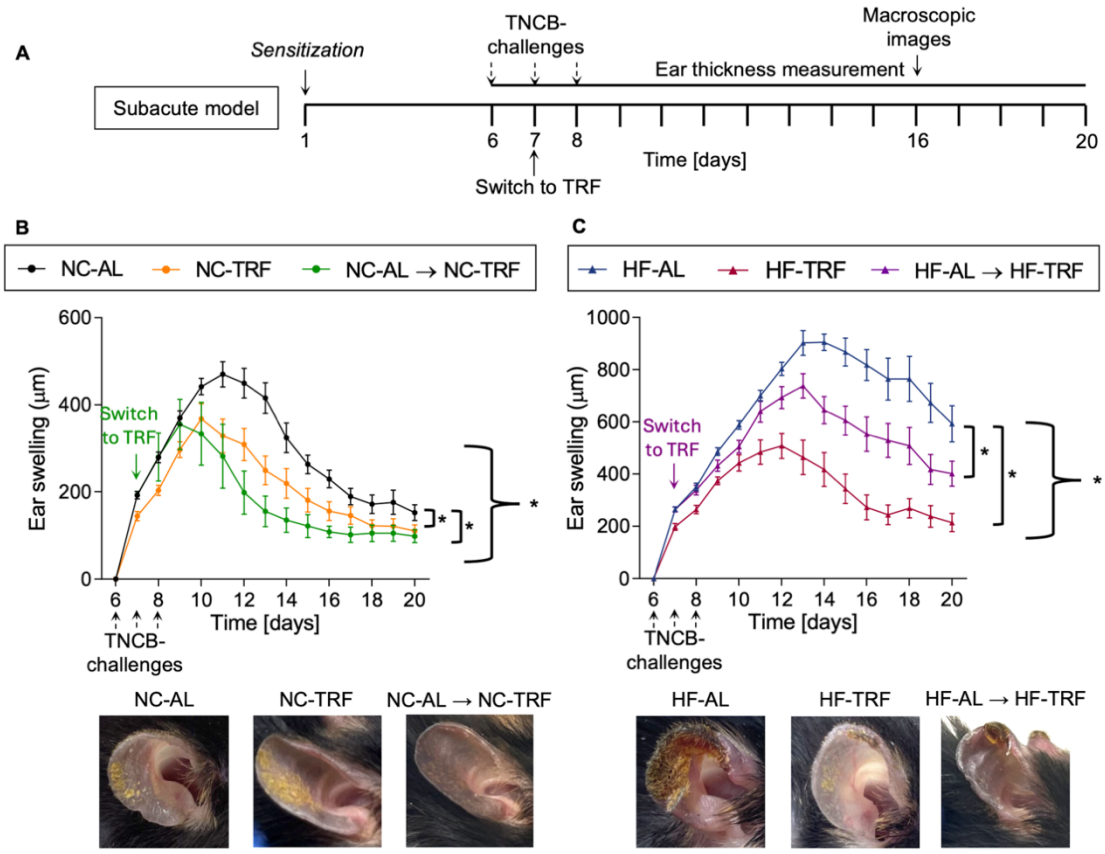

*Figure 23. Preventive and therapeutic effect of TRF on recovery from CHS in the subacute model of the disease. (A) Schematic outline of the CHS subacute model. Multiple ear challenges and a group of mice originally subjected to AL feeding were switched to TRF on day 7 are indicated. (B) Both preventive and therapeutic NC-TRF groups significantly improve recovery in the subacute model of CHS. Upper panel: Ear thickness normalized to data obtained on day 6. Mean ± SEM, n(NC-AL)=8-17, n(NC-TRF)=7-10, n(NC-AL → NC-TRF)=3. Repeated measures ANOVA (day 8 - day 16), significant group and group x time effect, *p<0.05. Lower panel: Representative macroscopic images of the ears from the indicated groups, taken 10 days after the TNCB challenge. (C) HF-AL feeding profoundly delays recovery, whereas TRF alleviates CHS severity in the subacute model. Upper panel: Ear thickness normalized to data obtained on day 6. Mean ± SEM, n(HF-AL)=11-19, n(HF-TRF)=11-14, n(HF-AL → HF-TRF)=10. Repeated measures ANOVA (day 8 - day 20), significant group and group x time effect, *p<0.05. Lower panel: Representative macroscopic images of the ears from the indicated groups, taken 10 days after the TNCB challenge.*

To assess how already developed inflammation affects food intake and how this is influenced by changes in the feeding schedule, we measured daily caloric intake. Under NC conditions, caloric intake was consistent throughout the entire period, and no differences between the groups were observed (Figure 24A). Under HF conditions, food intake rapidly decreased after the AL-TRF transition and remained at the level of the TRF

group (Figure 24B). In summary, food intake was dependent on both food composition and feeding schedule, even during inflammation.

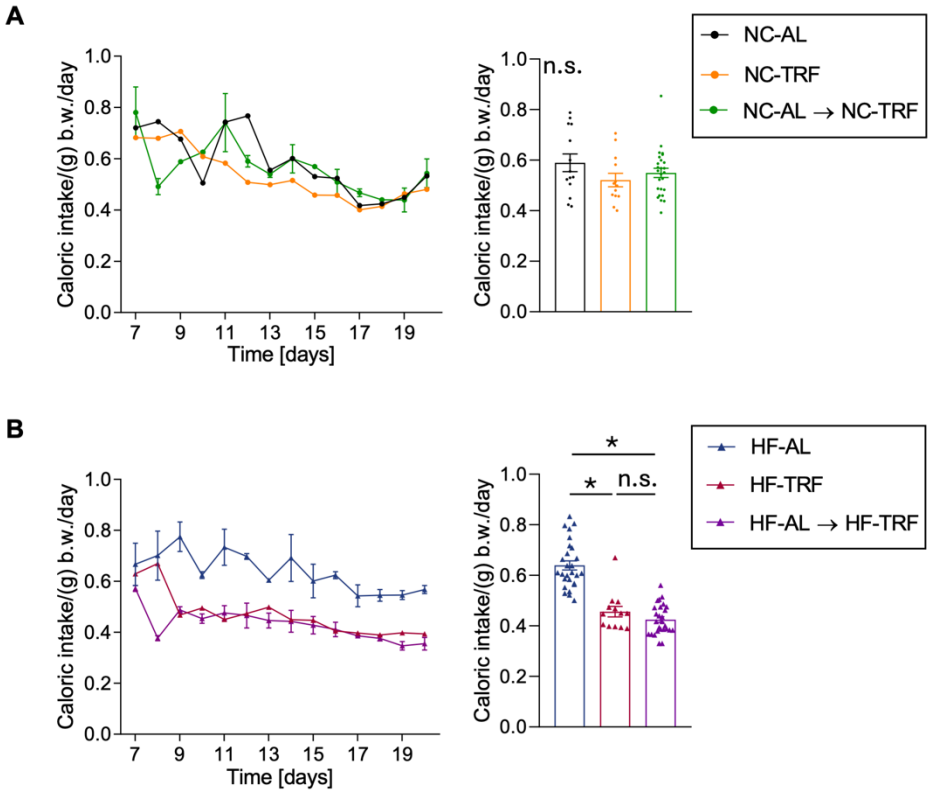

*Figure 24. Metabolic alterations under the subacute model of CHS. (A) Caloric intake of the NC-fed experimental groups during the subacute model. Food consumption was recorded daily. Data were normalized to g body weight. The left panel shows daily caloric intake, while the right panel presents the average daily intake over the recovery period. Mean ± SEM, n(NC-AL)cages=1, n(NC-TRF)cages=1, n(NC-AL→NC-TRF)cages=2. One-way ANOVA, no significant (n.s.) differences, *p<0.05. (B) HF-TRF groups decrease caloric intake under subacute inflammatory conditions. Food consumption was recorded daily. Data were normalized to g body weight. The left panel shows daily caloric intake, while the right panel presents the average daily intake over the recovery period. n(HF-AL)cages=2, n(HF-TRF) cages=1, n(HF-AL→HF-TRF)cages=2. One-way ANOVA, significant group effect, *p<0.05.*

We hypothesized that diet-induced exacerbation of inflammation is mediated by metabolic reorganization. As steady-state leptin levels (Figure 12) substantially reflect metabolic state and leptin has multiple effects on immune functions, we measured its levels in ear lysates on day 7 (Figure 25). HF diet significantly elevated leptin levels in the ear of both non-sensitized and sensitized groups; however, TRF counteracted this effect.

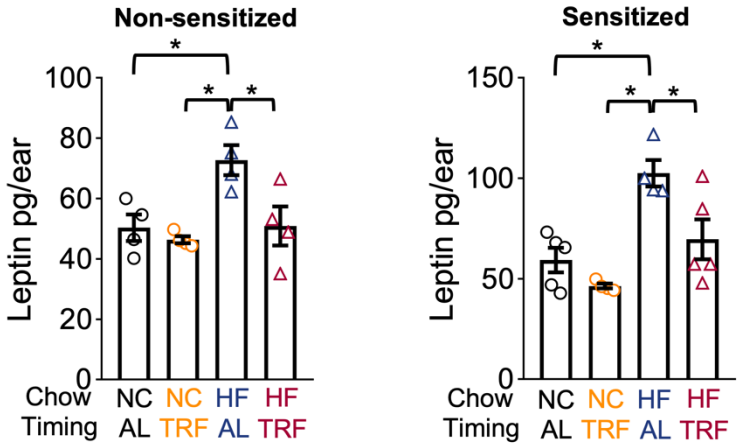

*Figure 25. Elevated tissue leptin levels in both non-sensitized (left panel) and sensitized (right panel) HF-AL mice. Tissue lysates were prepared from samples collected on day 7 of CHS. Mean ± SEM, non-sensitized: n(NC-AL)=4, n(NC-TRF)=4, n(HF-AL)=4, n(HF-TRF)=4, sensitized: n(NC-AL)=5, n(NC-TRF)=4, n(HF-AL)=4, n(HF-TRF)=5. One-way ANOVA, Post Hoc Tukey's HSD unequal N test, *p<0.05, significant group effect.*

4.3.3 Human pustulosis and leptin receptor expression

Based on the co-occurrence of elevated leptin levels and pustule formation, and to explore the human pathological relevance of our observations, we analyzed the transcriptomic data of PBMC samples from healthy control subjects and patients with generalized pustular psoriasis or psoriasis vulgaris (GSE200977) (121) for leptin receptor expression (Figure 26). The significantly higher LepR transcript levels in the samples of patients with generalized pustular psoriasis compared to controls suggest that leptin may contribute to the pathogenesis of pustulosis in human.

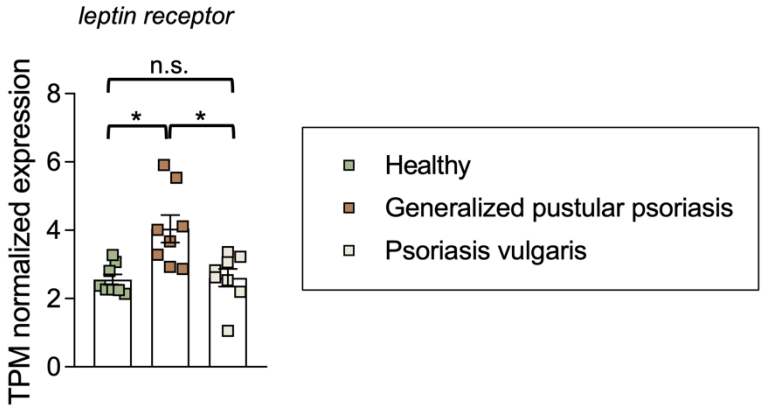

*Figure 26 Expression of leptin receptor is increased in patients with generalized pustular psoriasis compared to either healthy subjects or patients with psoriasis vulgaris. Human transcriptomic data were obtained from PBMC sample. Leptin receptor expression was normalized to TPM (transcripts per million). Mean ± SEM, n=8, One-way ANOVA, Post Hoc Tukey's HSD test, *p<0.05, significant group effect.*

4.3.4 The role of leptin in CHS

We hypothesized that the increased leptin levels in the ears, and, consequently, intraepidermal accumulation of neutrophils could contribute to the exacerbation of CHS in HF-fed animals. To investigate the possible role of leptin in CHS development, *db/db* mice - with a loss of function point mutation of the long form of leptin receptor (ObRb) - were used in the next experiments (Figure 27A). NC-AL-fed *db/db* mice, as a model with extremely elevated leptin production, have similar inflammatory processes to those of HF-AL animals, indicating that leptin may contribute to CHS severity, even acting through the short forms of the leptin receptors. Ear thickness of the *db/db* mice was slightly elevated compared to wild type littermates, and neutrophil counts, CXCL2, and IL-1ß levels were increased (Figure 27B-D). These results are associated with enhanced pustulosis in these animals.

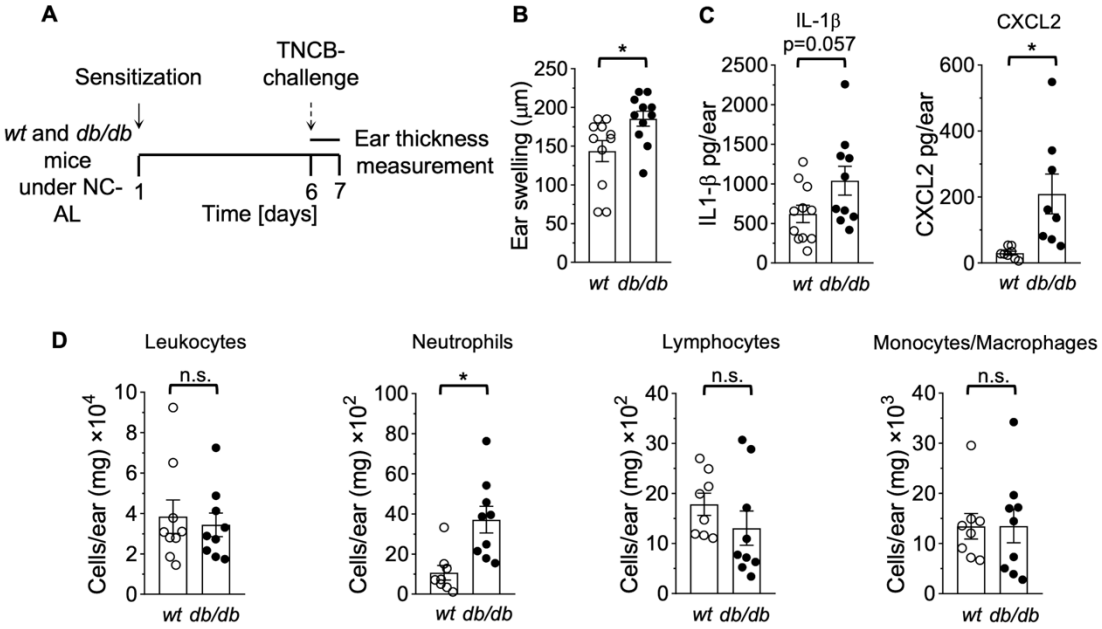

*Figure 27. Db/db mice exacerbate CHS reaction. (A) Experimental design for induction and following CHS in the C57BLKSDock7^{m}Lepr^{db} mouse strain. (B) Relative changes of ear thickness (day 7 - day 6) of wt and db/db mice following CHS induction. Mean ± SEM, n(wt)=11, n(db/db)=12, two-sample Student's t-test. (C) IL-1β and CXCL2 levels in lysates of inflamed ears of wt and db/db mice. Mean ± SEM n(wt)=8-11, n(db/db)=8-10, two-sample Student's t-test, *p<0.05. (D) Neutrophil accumulation in the ear is leptin dependent. Indicated immune cell counts were determined in lysates of inflamed ears of wt and db/db animals. Mean ± SEM, n(wt)=8-9, n(db/db)=9, two-sample Student's t-test, *p<0.05, n.s not significant.*

To further investigate the role of leptin in this inflammatory model, leptin receptor antagonist Allo-aca was applied intradermally to one ear, while vehicle was injected into the other ear. Blockade of LepR resulted in a reduction of ear swelling in *db/db* mice, suggesting that elevated leptin levels might have aggravated CHS (Figure 28).

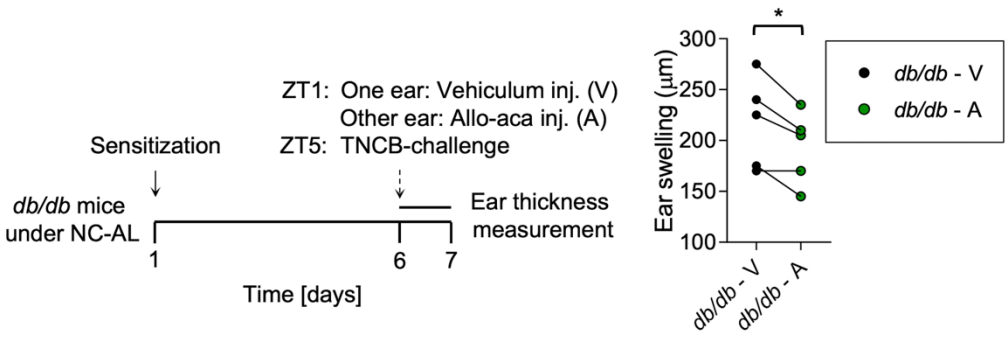

*Figure 28. Treatment with leptin receptor antagonist reduces ear swelling compared to control ears. Left panel: Experimental design. One ear of db/db mice was treated with vehicle, while the other with Allo-aca. Right panel: Ear thickness on day 7 was normalized to that on day 6. Data originating from vehicle- and Allo-aca-treated ears of the same animal are connected. n=5, paired Student's t-test, *p<0.05.*

To assess leptin's effect on allergic responses, CHS was induced in HF-AL mice in together with the administration of leptin receptor antagonist (Figure 29A). This self-controlled study shows that Allo-aca treatment resulted in a decrease in all measured inflammatory indicators (Figure 29B-D). Ear swelling was significantly reduced, while CXCL2 and IL-1ß levels were tendentiously reduced. Monocyte and neutrophil counts in ear lysates decreased in line with reduced pustule formation. These data also support our hypothesis that leptin contributes to the worsening of symptoms under HF-AL conditions.

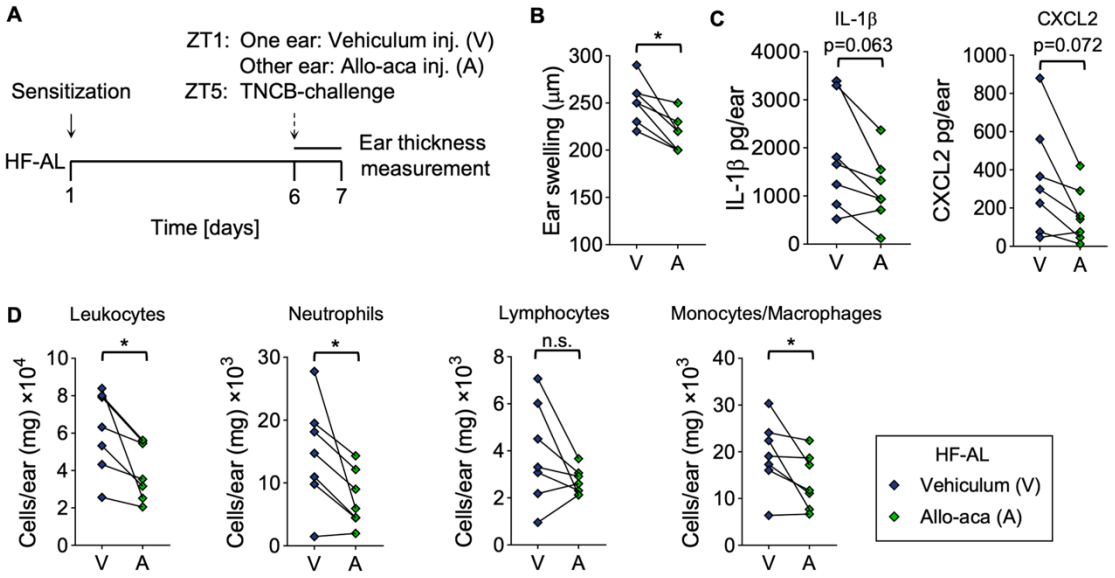

*Figure 29. Leptin receptor blocking alleviates CHS in HF-AL mice. (A) Experimental design of leptin receptor blocking with Allo-aca. One ear of HF-AL mice was treated with vehicle, while the other ear was administered Allo-aca. (B) Ear swelling in HF-AL mice is reduced by Allo-aca. Ear thickness on day 7 was normalized to that on day 6. Data originating from vehicle- and Allo-aca treated ears of the same animal are connected. n=7, paired Student's t-test, *p<0.05. (C) Effect of Allo-aca treatment on cytokine production in the inflamed tissues. IL-1β and CXCL2 levels were measured in lysates of vehicle- and Allo-aca treated ears. n=7, paired Student's t-test, *p<0.05. (D) Allo-aca affects leukocyte accumulation in the inflamed ears. Counts of the indicated cell types were determined in lysates of vehicle- and Allo-aca treated ears. n=7, paired Student's t-test, *p<0.05.*

5. DISCUSSION

Irregular eating patterns, such as late-night snacking, have emerged as a growing medical concern due to their contribution to the development of metabolic disorders. Given the bidirectional communication between metabolic and immune systems, impaired metabolic state is often linked to immune dysfunction, and an increased risk of exaggerated immune responses. For instance, the severity of rheumatoid arthritis correlates with body mass index (122), and generalized pustular psoriasis is comorbid with obesity in approximately 43% of the cases (123).

Conversely, well-synchronized meal timing has demonstrated both preventive and therapeutic potential for improving metabolic health and promoting longevity (27, 35). Time-restricted feeding increases thermogenesis rate and provides a sustainable approach for body weight management (36). In our study, the caloric intake of animals subjected to a HF diet was elevated. Due to adaptation to HF chow, HF groups decreased caloric intake in the second 2-week period. The difference in weight gain among the groups was less than 7%, considering a mild effect of the diet change on body weight. Consistent with findings by Hatori et al. (28), we observed that the HF-AL group consumed approximately twice as many calories as the NC-AL group during the inactive phase, suggesting greater circadian disruption of the metabolism in the HF-AL group. In addition, fasting blood glucose levels were slightly elevated in the HF groups, but the intraperitoneal glucose tolerance test showed no difference between groups. Similar IPGTT results were reported after four-week of high fat diet (124). Our findings support that HF diet impairs metabolic rhythmicity, whereas beneficial effects of TRF, even without caloric restriction, are observed on basic metabolic parameters both in NC and HF groups. Our study demonstrates that even a short-term TRF effectively regulates energy storage and expenditure. Furthermore, the significance of temporal regulation may likely extends beyond metabolism to the regulation of hormonal homeostasis. In line with this, the HF diet induced a phase shift in the circadian rhythm of serum corticosterone, resulting in a phase advance with an acrophase during the light phase. Interestingly, Kohsaka et al showed that a high-fat diet decreased the daily amplitude of corticosterone concentrations without causing a phase shift (44). However, the average daily corticosterone levels did not differ significantly among the experimental groups,

indicating that the phase advance induced by the HF diet reflects a physiological adaptation in the metabolic regulation rather than a stress response.

To further explore how TRF affects metabolic functions, our investigations focused on the circadian rhythm of metabolic organs, particularly adipose tissue. Adipocyte clock genes exhibited stronger rhythmicity, and the daily average gene expression level of inflammatory cytokines (*tnfα, nlrp3, il18*) and adipokines (*adipsin* and *leptin*) was reduced. Parallelly, leptin rhythmicity was enhanced by TRF. HF attenuated clock genes' transcript levels (*per1, per3*) and elevated *leptin* expression, - effects that were prevented by TRF. Systemic serum leptin levels correlate with adipose tissue mass and are influenced by feeding behavior: leptin peaks during the active (dark) phase in mice on normal chow. However, this rhythm was advanced in HF-AL animals. In contrast, HF-TRF prevented these alterations and restored leptin levels and rhythmicity. Adipose tissue-derived leptin may also modulate the activation and priming of immune cells (104, 105). At ZT1, TRF led to reduced expression of adhesion molecules and chemokine receptors (CD49d, CD29, CD11b, CXCR4) on peripheral blood neutrophils and monocytes, which correlated with decreased serum leptin levels (66). In turn, a high-fat diet increased the daily average of CD11b expression and elevated leptin levels at all timepoints. In *ex vivo* experiments, leptin-treated peripheral blood myeloid cells (isolated from NC-AL mice at ZT1) showed increased integrin and chemokine expression. Taken together, these findings indicate that circulating leptin predisposes immune cells to enhanced migratory capacity. Importantly, elevated leptin levels were associated with increased severity of both rheumatoid arthritis and contact hypersensitivity, whereas TRF mitigated these negative effects regardless of the diet. Aggravating effect of HF on CHS has been previously reported (125), therefore, this part of our observations is only an independent confirmation of previous data. However, we also showed that HF diet worsened the severity of CHS in both non-sensitized and sensitized animals, indicating that HF enhances immune responsiveness and contributes to both irritant and allergic contact dermatitis. This effect is primarily driven by infiltrating neutrophils, as supported by increased tissue CXCL2 levels, histological analysis, and absolute neutrophil counts. Further supporting leptin's local effects, we observed elevated leptin levels in inflamed tissue, likely due to increased vascular permeability. Locally, leptin may stimulate keratinocytes to secrete CXCL2 and other key chemoattractants (126). It also enhances

Th17 differentiation and the production of IL-17, amplifying inflammation (98). Moreover, contact hypersensitivity reaction was reduced due to administration of leptin receptor antagonist in both *db/db* and *wild type* HF-AL mice, further implicating the leptin-leptin receptor axis in disease severity. Overall, a high-fat diet promotes adipose tissue dysfunction and chronic leptin elevation, whereas TRF appears to exert anti-inflammatory effects via leptin reduction. We propose that leptin rhythmicity regulates leukocyte priming: high leptin levels during the active phase promote immune cell activation and tissue migration, while low leptin levels coincide with immune cell homing during the inactive phase. That means that *ad libitum* food intake-induced leptin level elevation during the inactive phase associates with opposing the demands of the immune system: mistimed activation of the immune cells, even under "steady-state", - a scenario we interpret as a state of low-grade inflammation. On the other hand, increased serum leptin levels are associated with a higher number of infiltrated myeloid cells into the inflammation site following inflammatory challenge. We propose that HF diet-induced leptin elevation contributes to the exacerbation of inflammation by promoting the priming and migration of myeloid cells (Figure 30); but not the initiation of the inflammatory response itself. In line with this, TRF and locally applied leptin receptor antagonist alleviate inflammation severity (Figure 30). Moreover, leptin receptor expression is elevated in human PBMC samples from patients with generalized pustular psoriasis, indicating potential further translational relevance of our observations and highlighting leptin as a therapeutic target.

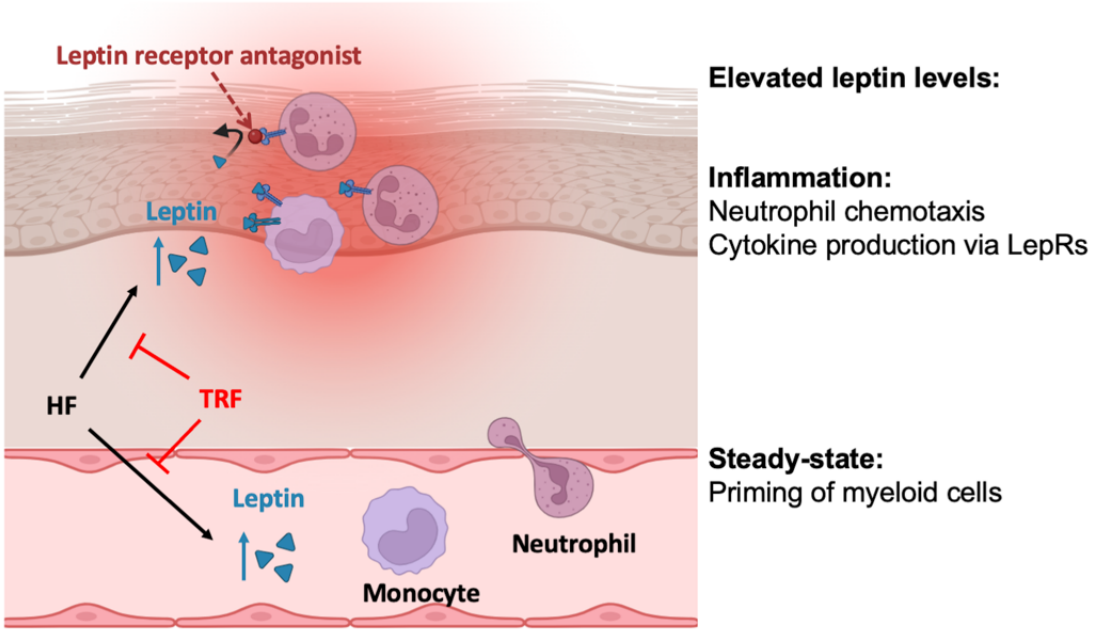

Figure 30 Dual role of leptin and the impact of its blockade. Our findings demonstrate that HF diet-induced leptin production elevates serum leptin levels, activating myeloid cells under steady-state conditions. Inflammation initiates the extravasation of plasma proteins, including leptin, at inflammation sites, triggering immune cell chemotaxis and further promoting their tissue migration. Leptin level is decreased by high-fat time-restricted feeding (TRF), resulting inflammation-attenuation. In our study, the intradermal administration of a leptin receptor antagonist effectively inhibited leptin's proinflammatory effects, including the reduction of neutrophil accumulation in the skin.

Beyond leptin, the gut microbiome also plays a key role in diet-induced immune changes. While our study did not directly examine the gut microbiota, we took into account its well-established role in mediating the effects of diet on immune regulation. Previous studies have clearly demonstrated that high-fat diets negatively impact the gut microbiome, which serves as a crucial interface between nutrition and immunity. In the context of obesity, microbial diversity is reduced, and community composition becomes altered. High-fat diets induce intestinal dysbiosis (127), impair epithelial barrier integrity, and increase gut permeability (127). Consequently, bacterial translocation occurs across the intestinal epithelium, leading to elevated plasma levels of lipopolysaccharide (LPS) and interleukin-17 (IL-17), both of which are associated with weight gain and enhanced systemic inflammation. Furthermore, high-fat-fed mice lacking IL-17A specifically in intestinal epithelial cells exhibit significantly lower serum leptin levels compared to wild-type controls on the same high-fat diet, although leptin levels remain elevated relative to

mice on a normal diet (128, 129), indicating an alternative, additive mechanism to those we identified in our study.

Taken together, these negative effects of high-fat diet on metabolic and immune function can be mitigated by time-restricted feeding. To our knowledge, our experiment with the subacute regeneration of CHS was the first study to demonstrate TRF as a therapeutic approach to attenuate inflammatory response, regardless of chow type. Our data suggest that the human translation of our model, TRE, might offer similar benefits in the prevention and treatment of allergic skin diseases. Furthermore, GPP and AGEP are often triggered by drug side effects or infections, suggesting that TRE could be applied alongside pharmacological treatments to reduce the incidence of these side effects and also improve patients' metabolic status and inflammation outcome. However, further investigations, like interactions between TRE and drug pharmacokinetics/dynamics, are necessary. In the context of clinical trials assessing TRE, whether as a monotherapy or in combination with pharmacological agents, it is essential to evaluate pharmacokinetic and pharmacodynamic parameters, including absorption, distribution, metabolism, elimination, and toxicity (130). These processes may be modulated by TRE through its effects on peripheral circadian clocks.

Furthermore, our observations open up the possibility that timed food intake, through enhancing the rhythms of leptin and leukocytes, may also exert systemic immunomodulatory actions with relevance to host defense. As we previously proposed, TRF enhances leukocyte rhythmicity, implying that a greater number of leukocytes are distributed throughout peripheral tissues and primed to combat pathogenic insults during the active phase (66). Circadian-immune researchers should further examine the potential effects of TRF and TRE on host defense mechanisms. We hypothesize that TRE, when employed as a complementary therapy alongside conventional bactericidal agents, may improve infection clearance while simultaneously mitigating adverse effects such as GPP or AGEP. Moreover, TRE may offer therapeutic benefits in the context of autoimmune disorders, such as rheumatoid arthritis. Specifically, TRE may enhance the efficacy of DMARDs, particularly in the reduction of symptom severity, and potentially lower the infection risk.

While these immunomodulatory perspectives remain to be fully explored, our findings already establish a compelling foundation for temporally controlled feeding strategies as tools to modulate metabolic and inflammatory pathways. This conceptual framework now converges into a practical take-home message:

A 10-hour feeding window aligned with light-dark cycles improves metabolic health and maintains body weight. Short-term dietary intervention induces metabolic reorganization, clearly reflected by significant changes in serum leptin levels. The observed anti-inflammatory effects of both time-restricted feeding and local leptin receptor blockade underscore the translational potential of our study, offering promising new avenues for the therapy of inflammatory diseases such as rheumatoid arthritis and allergic contact dermatitis.

6. CONCLUSIONS

1. Short-term time-restricted feeding improved metabolic rhythms under both normal and high-fat diets. Remarkably, TRF prevented body weight gain despite similar caloric intake compared to *ad libitum* groups. HF groups showed mild disruption of glucose homeostasis: fasting glucose levels were elevated, while glucose tolerance remained unaffected compared to the other experimental groups. The corticosterone rhythm was phase-shifted among groups, but the average hormone levels did not differ significantly.
2. The NC-TRF group showed significantly lower expression levels of inflammatory mediators (*il-18, nlrp3, tnfα, il-6* and *adipsin*) compared to NC-AL, suggesting an anti-inflammatory effect of TRF in white adipose tissue. Regarding the clock genes and leptin expression, HF disrupted, whereas TRF preserved the robust amplitude of *per1, per3, dbp,* and *leptin* rhythm. Consequently, serum leptin levels were lower during the day and retained rhythmicity in the TRF groups, whereas AL feeding blunted leptin oscillation.
3. HF diet elevated CD11b levels on the surface of neutrophils and monocytes in the peripheral blood, an effect reversed by TRF. Furthermore, *ex vivo* leptin treatment upregulated adhesion molecule expression (CD62L, CD29, CD49d, and CXCR4).
4. TRF significantly reduced arthritis severity, as evidenced by clinical scores, grip strength tests, and immune cell analysis. Additionally, HF diet increased neutrophil migratory potential.
5. HF worsened, whereas TRF ameliorated acute contact hypersensitivity. Tissue neutrophil count, IL-1β, CXCL2, and leptin levels correlated positively with CHS severity. We hypothesized that leptin exacerbates inflammation via neutrophil recruitment. Our results show anti-inflammatory effects of leptin receptor blockade in the acute CHS model, both on *db/db* and *wt* HF-AL mice. Furthermore, our study reveals the preventive and therapeutic potential of TRF in both acute and subacute CHS models.

Our findings and their potential translation into clinical practice may provide novel insights into prevention and treatment of rheumatoid arthritis and contact dermatitis.

7. SUMMARY

In modern societies, irregular and unhealthy eating patterns are increasingly prevalent, contributing to the development of both metabolic and inflammatory disorders. Restricting food access to a specific time window of the day, even without reducing caloric intake, entrains peripheral clocks and enhances metabolic rhythm. Timed food intake represents an affordable and well-tolerable approach that is beneficial for both the prevention and treatment of metabolic diseases. Bidirectional communication between metabolism and immunity suggests that time-restricted eating may serve as a complementary therapy for inflammatory diseases as well.

We addressed the metabolic effect of different feeding regimens, like *ad libitum* (AL) and time-restricted feeding (TRF) subjected to both normal chow (NC) and high-fat (HF) diet under steady-state conditions. HF-AL impairs metabolic state, leads to excessive body mass increase, elevated fasting glucose levels, phase-shifted corticosterone rhythms, and increased serum leptin levels. HF-TRF partially prevents these negative effects, potentially through the synchronization of the white adipose tissue clock.

We investigated how the timing of food intake influences K/BxN serum-transfer arthritis (STA) and contact hypersensitivity (CHS), a mouse model of human rheumatoid arthritis (RA) and allergic contact dermatitis (ACD), respectively. Inflammation was analyzed at the macroscopic, tissue, and cellular levels. In the group with AL food access, the HF diet worsened the inflammatory response, as indicated by increased inflammatory swelling, neutrophil infiltration, IL-1β, and leptin levels compared to NC conditions. NC-fed *db/db* mice that produced high levels of leptin exhibited worsened CHS. Moreover, blocking the leptin receptors alleviated the phenotypic and molecular signs of inflammation in *db/db*, as well as in HF-AL mice.

Our data indicate that HF diet and prolonged daily eating periods can exacerbate inflammatory responses in various disease models. According to our model, leptin might contribute to the pathogenesis by promoting the activity of circulating myeloid cells via increasing adhesion molecule expression under steady-state conditions and enhancing their migratory capacity under inflammatory conditions. Based on our results, the inflammation-attenuating effect of both TRF and local inhibition of leptin receptors may offer promising therapeutic strategies for managing RA and ACD.

8. REFERENCES

1. Lee DY, Jung I, Park SY, Yu JH, Seo JA, Kim KJ, et al. Attention to Innate Circadian Rhythm and the Impact of Its Disruption on Diabetes. Diabetes Metab J. 2024;48(1):37-52.
2. Eastman CI, Suh C, Tomaka VA, Crowley SJ. Circadian rhythm phase shifts and endogenous free-running circadian period differ between African-Americans and European-Americans. Sci Rep. 2015;5:8381.
3. Eckel-Mahan K, Sassone-Corsi P. Phenotyping Circadian Rhythms in Mice. Curr Protoc Mouse Biol. 2015;5(3):271-81.
4. Bargiello TA, Jackson FR, Young MW. Restoration of circadian behavioural rhythms by gene transfer in Drosophila. Nature. 1984;312(5996):752-4.
5. Zehring WA, Wheeler DA, Reddy P, Konopka RJ, Kyriacou CP, Rosbash M, et al. P-element transformation with period locus DNA restores rhythmicity to mutant, arrhythmic Drosophila melanogaster. Cell. 1984;39(2 Pt 1):369-76.
6. Hardin PE, Hall JC, Rosbash M. Feedback of the Drosophila period gene product on circadian cycling of its messenger RNA levels. Nature. 1990;343(6258):536-40.
7. Takahashi JS. Transcriptional architecture of the mammalian circadian clock. Nat Rev Genet. 2017;18(3):164-79.
8. Mure LS, Le HD, Benegiamo G, Chang MW, Rios L, Jillani N, et al. Diurnal transcriptome atlas of a primate across major neural and peripheral tissues. Science. 2018;359(6381).
9. Sancar A, Lindsey-Boltz LA, Kang TH, Reardon JT, Lee JH, Ozturk N. Circadian clock control of the cellular response to DNA damage. FEBS Lett. 2010;584(12):2618-25.
10. Pandi-Perumal SR, Cardinali DP, Zaki NFW, Karthikeyan R, Spence DW, Reiter RJ, et al. Timing is everything: Circadian rhythms and their role in the control of sleep. Front Neuroendocrinol. 2022;66:100978.
11. Refinetti R. Circadian rhythmicity of body temperature and metabolism. Temperature (Austin). 2020;7(4):321-62.
12. Sato T, Sato S. Circadian Regulation of Metabolism: Commitment to Health and Diseases. Endocrinology. 2023;164(7).

13. Claustrat B, Leston J. Melatonin: Physiological effects in humans. Neurochirurgie. 2015;61(2-3):77-84.
14. Douma LG, Gumz ML. Circadian clock-mediated regulation of blood pressure. Free Radic Biol Med. 2018;119:108-14.
15. Hughes ATL, Piggins HD. Feedback actions of locomotor activity to the circadian clock. Prog Brain Res. 2012;199:305-36.
16. Xu Y, Toh KL, Jones CR, Shin JY, Fu YH, Ptacek LJ. Modeling of a human circadian mutation yields insights into clock regulation by PER2. Cell. 2007;128(1):59-70.
17. Patke A, Murphy PJ, Onat OE, Krieger AC, Ozcelik T, Campbell SS, et al. Mutation of the Human Circadian Clock Gene CRY1 in Familial Delayed Sleep Phase Disorder. Cell. 2017;169(2):203-15 e13.
18. Ko CH, Takahashi JS. Molecular components of the mammalian circadian clock. Hum Mol Genet. 2006;15 Spec No 2:R271-7.
19. Janoski JR, Aiello I, Lundberg CW, Finkielstein CV. Circadian clock gene polymorphisms implicated in human pathologies. Trends Genet. 2024;40(10):834-52.
20. Sudy AR, Ella K, Bodizs R, Kaldi K. Association of Social Jetlag With Sleep Quality and Autonomic Cardiac Control During Sleep in Young Healthy Men. Front Neurosci. 2019;13:950.
21. Santos I, Rocha I, Gozal D, Meira ECM. Obstructive sleep apnea, shift work and cardiometabolic risk. Sleep Med. 2020;74:132-40.
22. Szkiela M, Kusidel E, Makowiec-Dabrowska T, Kaleta D. How the Intensity of Night Shift Work Affects Breast Cancer Risk. Int J Environ Res Public Health. 2021;18(9).
23. Thomas J, Overeem S, Dresler M, Kessels RPC, Claassen J. Shift-work-related sleep disruption and the risk of decline in cognitive function: The CRUISE Study. J Sleep Res. 2021;30(2):e13068.
24. Thorkildsen MS, Gustad LT, Damas JK. The Effects of Shift Work on the Immune System: A Narrative Review. Sleep Sci. 2023;16(3):e368-e74.
25. Xu M, Yin X, Gong Y. Lifestyle Factors in the Association of Shift Work and Depression and Anxiety. JAMA Netw Open. 2023;6(8):e2328798.

26. Zhang H, Wang J, Zhang S, Tong S, Hu J, Che Y, et al. Relationship between night shift and sleep problems, risk of metabolic abnormalities of nurses: a 2 years follow-up retrospective analysis in the National Nurse Health Study (NNHS). Int Arch Occup Environ Health. 2023;96(10):1361-71.
27. Manoogian ENC, Panda S. Circadian rhythms, time-restricted feeding, and healthy aging. Ageing Res Rev. 2017;39:59-67.
28. Hatori M, Vollmers C, Zarrinpar A, DiTacchio L, Bushong EA, Gill S, et al. Time-restricted feeding without reducing caloric intake prevents metabolic diseases in mice fed a high-fat diet. Cell Metab. 2012;15(6):848-60.
29. Kolbe I, Husse J, Salinas G, Lingner T, Astiz M, Oster H. The SCN Clock Governs Circadian Transcription Rhythms in Murine Epididymal White Adipose Tissue. J Biol Rhythms. 2016;31(6):577-87.
30. Van Der Spek R, Foppen E, Fliers E, La Fleur S, Kalsbeek A. Thermal lesions of the SCN do not abolish all gene expression rhythms in rat white adipose tissue, NAMPT remains rhythmic. Chronobiol Int. 2021;38(9):1354-66.
31. Bass J. Interorgan rhythmicity as a feature of healthful metabolism. Cell Metab. 2024;36(4):655-69.
32. Gagliano O, Luni C, Li Y, Angiolillo S, Qin W, Panariello F, et al. Synchronization between peripheral circadian clock and feeding-fasting cycles in microfluidic device sustains oscillatory pattern of transcriptome. Nat Commun. 2021;12(1):6185.
33. Heyde I, Begemann K, Oster H. Contributions of white and brown adipose tissues to the circadian regulation of energy metabolism. Endocrinology. 2021;162(3).
34. Hara R, Wan K, Wakamatsu H, Aida R, Moriya T, Akiyama M, et al. Restricted feeding entrains liver clock without participation of the suprachiasmatic nucleus. Genes Cells. 2001;6(3):269-78.
35. Longo VD, Panda S. Fasting, Circadian Rhythms, and Time-Restricted Feeding in Healthy Lifespan. Cell Metab. 2016;23(6):1048-59.
36. Hepler C, Weidemann BJ, Waldeck NJ, Marcheva B, Cedernaes J, Thorne AK, et al. Time-restricted feeding mitigates obesity through adipocyte thermogenesis. Science. 2022;378(6617):276-84.

37. Chang YJ, Turner L, Teong XT, Zhao L, Variji A, Wittert GA, et al. Comparing the effectiveness of calorie restriction with and without time-restricted eating on the circadian regulation of metabolism: rationale and protocol of a three-arm randomised controlled trial in adults at risk of type 2 diabetes. Nutr Res. 2025;138:33-44.
38. Johnson SL, Murray G, Manoogian ENC, Mason L, Allen JD, Berk M, et al. A pre-post trial to examine biological mechanisms of the effects of time-restricted eating on symptoms and quality of life in bipolar disorder. BMC Psychiatry. 2024;24(1):711.
39. Kleckner AS, Clingan CL, Youngblood SM, Kleckner IR, Quick L, Elrod RD, et al. Time-restricted eating to address persistent cancer-related fatigue among cancer survivors: a randomized controlled trial. Support Care Cancer. 2025;33(4):353.
40. Manoogian ENC, Wilkinson MJ, O'Neal M, Laing K, Nguyen J, Van D, et al. Time-Restricted Eating in Adults With Metabolic Syndrome : A Randomized Controlled Trial. Ann Intern Med. 2024;177(11):1462-70.
41. Papageorgiou M, Biver E, Mareschal J, Phillips NE, Hemmer A, Biolley E, et al. The effects of time-restricted eating and weight loss on bone metabolism and health: a 6-month randomized controlled trial. Obesity (Silver Spring). 2023;31 Suppl 1(Suppl 1):85-95.
42. Santos-Baez LS, Diaz-Rizzolo DA, Borhan R, Popp CJ, Sordi-Guth A, DeBonis D, et al. Predictive models of post-prandial glucose response in persons with prediabetes and early onset type 2 diabetes: A pilot study. Diabetes Obes Metab. 2025;27(3):1515-25.
43. Termannsen AD, Varming A, Bjerre N, Wodschow HZ, Hansen GS, Jensen NJ, et al. Protocol for a 1-year randomised, controlled, parallel group, open-label trial on the effects and feasibility of time-restricted eating in individuals with type 2 diabetes- The REStricted Eating Time in the treatment of type 2 diabetes (RESET2) trial. Diabet Med. 2025;42(5):e15506.
44. Kohsaka A, Laposky AD, Ramsey KM, Estrada C, Joshu C, Kobayashi Y, et al. High-fat diet disrupts behavioral and molecular circadian rhythms in mice. Cell Metab. 2007;6(5):414-21.

45. Lazarescu O, Ziv-Agam M, Haim Y, Hekselman I, Jubran J, Shneyour A, et al. Human subcutaneous and visceral adipocyte atlases uncover classical and nonclassical adipocytes and depot-specific patterns. Nat Genet. 2025;57(2):413-26.
46. Douglas A, Stevens B, Rendas M, Kane H, Lynch E, Kunkemoeller B, et al. Rhythmic IL-17 production by gammadelta T cells maintains adipose de novo lipogenesis. Nature. 2024;636(8041):206-14.
47. Tilg H, Ianiro G, Gasbarrini A, Adolph TE. Adipokines: masterminds of metabolic inflammation. Nat Rev Immunol. 2025;25(4):250-65.
48. Sun M, Zhang Y, Guo A, Xia Z, Peng L. Progress in the Correlation Between Inflammasome NLRP3 and Liver Fibrosis. J Clin Transl Hepatol. 2024;12(2):191-200.
49. Kettner NM, Mayo SA, Hua J, Lee C, Moore DD, Fu L. Circadian Dysfunction Induces Leptin Resistance in Mice. Cell Metab. 2015;22(3):448-59.
50. Khan S, Chan YT, Revelo XS, Winer DA. The Immune Landscape of Visceral Adipose Tissue During Obesity and Aging. Front Endocrinol (Lausanne). 2020;11:267.
51. Kumari M, Heeren J, Scheja L. Regulation of immunometabolism in adipose tissue. Semin Immunopathol. 2018;40(2):189-202.
52. Nance SA, Muir L, Lumeng C. Adipose tissue macrophages: Regulators of adipose tissue immunometabolism during obesity. Mol Metab. 2022;66:101642.
53. Qi Y, Hui X. The shades of grey in adipose tissue reprogramming. Biosci Rep. 2022;42(3).
54. Leinweber B, Pilorz V, Olejniczak I, Skrum L, Begemann K, Heyde I, et al. Bmal1 deficiency in neutrophils alleviates symptoms induced by high-fat diet. iScience. 2025;28(3):112038.
55. Casanova-Acebes M, Pitaval C, Weiss LA, Nombela-Arrieta C, Chevre R, N AG, et al. Rhythmic modulation of the hematopoietic niche through neutrophil clearance. Cell. 2013;153(5):1025-35.
56. Scheiermann C, Kunisaki Y, Frenette PS. Circadian control of the immune system. Nat Rev Immunol. 2013;13(3):190-8.

57. Stenzinger M, Karpova D, Unterrainer C, Harenkamp S, Wiercinska E, Hoerster K, et al. Hematopoietic-Extrinsic Cues Dictate Circadian Redistribution of Mature and Immature Hematopoietic Cells in Blood and Spleen. Cells. 2019;8(9).
58. He W, Holtkamp S, Hergenhan SM, Kraus K, de Juan A, Weber J, et al. Circadian Expression of Migratory Factors Establishes Lineage-Specific Signatures that Guide the Homing of Leukocyte Subsets to Tissues. Immunity. 2018;49(6):1175-90 e7.
59. Pick R, He W, Chen CS, Scheiermann C. Time-of-Day-Dependent Trafficking and Function of Leukocyte Subsets. Trends Immunol. 2019;40(6):524-37.
60. Adrover JM, Del Fresno C, Crainiciuc G, Cuartero MI, Casanova-Acebes M, Weiss LA, et al. A Neutrophil Timer Coordinates Immune Defense and Vascular Protection. Immunity. 2019;50(2):390-402 e10.
61. Ella K, Csepanyi-Komi R, Kaldi K. Circadian regulation of human peripheral neutrophils. Brain Behav Immun. 2016;57:209-21.
62. Ovadia S, Ozcan A, Hidalgo A. The circadian neutrophil, inside-out. J Leukoc Biol. 2023;113(6):555-66.
63. Vicanolo T, Ozcan A, Li JL, Huerta-Lopez C, Ballesteros I, Rubio-Ponce A, et al. Matrix-producing neutrophils populate and shield the skin. Nature. 2025;641(8063):740-8.
64. Ella K, Mocsai A, Kaldi K. Circadian regulation of neutrophils: Control by a cell-autonomous clock or systemic factors? Eur J Clin Invest. 2018;48 Suppl 2:e12965.
65. Boro M, Balaji KN. CXCL1 and CXCL2 Regulate NLRP3 Inflammasome Activation via G-Protein-Coupled Receptor CXCR2. J Immunol. 2017;199(5):1660-71.
66. Ella K, Sudy AR, Bur Z, Koos B, Kisiczki AS, Mocsai A, et al. Time restricted feeding modifies leukocyte responsiveness and improves inflammation outcome. Front Immunol. 2022;13:924541.
67. Cross M, Smith E, Hoy D, Carmona L, Wolfe F, Vos T, et al. The global burden of rheumatoid arthritis: estimates from the global burden of disease 2010 study. Ann Rheum Dis. 2014;73(7):1316-22.

68. Crowson CS, Matteson EL, Myasoedova E, Michet CJ, Ernste FC, Warrington KJ, et al. The lifetime risk of adult-onset rheumatoid arthritis and other inflammatory autoimmune rheumatic diseases. Arthritis Rheum. 2011;63(3):633-9.
69. Romao VC, Fonseca JE. Etiology and Risk Factors for Rheumatoid Arthritis: A State-of-the-Art Review. Front Med (Lausanne). 2021;8:689698.
70. Gibbs JE, Ray DW. The role of the circadian clock in rheumatoid arthritis. Arthritis Res Ther. 2013;15(1):205.
71. Downton P, Dickson SH, Ray DW, Bechtold DA, Gibbs JE. Fibroblast-like synoviocytes orchestrate daily rhythmic inflammation in arthritis. Open Biol. 2024;14(7):240089.
72. Miyabe Y, Miyabe C, Iwai Y, Luster AD. Targeting the Chemokine System in Rheumatoid Arthritis and Vasculitis. JMA J. 2020;3(3):182-92.
73. Brand DD, Latham KA, Rosloniec EF. Collagen-induced arthritis. Nat Protoc. 2007;2(5):1269-75.
74. Liang J, Yang K, Shen Y, Peng X, Tan H, Liu L, et al. Incidence of collagen-induced arthritis is elevated by a high-fat diet without influencing body weight in mice. RMD Open. 2024;10(2).
75. Monach PA, Mathis D, Benoist C. The K/BxN arthritis model. Curr Protoc Immunol. 2008;Chapter 15:15 22 1-15 22 12.
76. Li Y, Zou W, Brestoff JR, Rohatgi N, Wu X, Atkinson JP, et al. Fat-Produced Adipsin Regulates Inflammatory Arthritis. Cell Rep. 2019;27(10):2809-16 e3.
77. Yamada H. Adaptive immunity in the joint of rheumatoid arthritis. Immunol Med. 2022;45(1):1-11.
78. Watts GM, Beurskens FJ, Martin-Padura I, Ballantyne CM, Klickstein LB, Brenner MB, et al. Manifestations of inflammatory arthritis are critically dependent on LFA-1. J Immunol. 2005;174(6):3668-75.
79. Smolen JS, Aletaha D, McInnes IB. Rheumatoid arthritis. Lancet. 2016;388(10055):2023-38.
80. Cutolo M. Glucocorticoids and chronotherapy in rheumatoid arthritis. RMD Open. 2016;2(1):e000203.

81. Giangreco D, Cutolo M. Morning glucocorticoids versus night glucocorticoids: the role of low-dose glucocorticoid chronotherapy in rheumatoid arthritis. J Clin Rheumatol. 2014;20(8):437-9.
82. Alinaghi F, Bennike NH, Egeberg A, Thyssen JP, Johansen JD. Prevalence of contact allergy in the general population: A systematic review and meta-analysis. Contact Dermatitis. 2019;80(2):77-85.
83. Fitzpatrick JM, Roberts DW, Patlewicz G. What determines skin sensitization potency: Myths, maybes and realities. The 500 molecular weight cut-off: An updated analysis. J Appl Toxicol. 2017;37(1):105-16.
84. Peiser M. Role of Th17 cells in skin inflammation of allergic contact dermatitis. Clin Dev Immunol. 2013;2013:261037.
85. Peiser M, Tralau T, Heidler J, Api AM, Arts JH, Basketter DA, et al. Allergic contact dermatitis: epidemiology, molecular mechanisms, in vitro methods and regulatory aspects. Current knowledge assembled at an international workshop at BfR, Germany. Cell Mol Life Sci. 2012;69(5):763-81.
86. Weber FC, Nemeth T, Csepregi JZ, Dudeck A, Roers A, Ozsvari B, et al. Neutrophils are required for both the sensitization and elicitation phase of contact hypersensitivity. J Exp Med. 2015;212(1):15-22.
87. Watanabe H, Gaide O, Petrilli V, Martinon F, Contassot E, Roques S, et al. Activation of the IL-1beta-processing inflammasome is involved in contact hypersensitivity. J Invest Dermatol. 2007;127(8):1956-63.
88. Nakae S, Komiyama Y, Nambu A, Sudo K, Iwase M, Homma I, et al. Antigen-specific T cell sensitization is impaired in IL-17-deficient mice, causing suppression of allergic cellular and humoral responses. Immunity. 2002;17(3):375-87.
89. Aradi P, Kovacs G, Kemecsei E, Molnar K, Sagi SM, Horvath Z, et al. Lymphatic-Dependent Modulation of the Sensitization and Elicitation Phases of Contact Hypersensitivity. J Invest Dermatol. 2024;144(10):2240-54 e9.
90. Miyake T, Egawa G, Chow Z, Asahina R, Otsuka M, Nakajima S, et al. Circadian rhythm affects the magnitude of contact hypersensitivity response in mice. Allergy. 2022;77(9):2748-59.

91. Takita E, Yokota S, Tahara Y, Hirao A, Aoki N, Nakamura Y, et al. Biological clock dysfunction exacerbates contact hypersensitivity in mice. Br J Dermatol. 2013;168(1):39-46.
92. Zhou X, Chen Y, Cui L, Shi Y, Guo C. Advances in the pathogenesis of psoriasis: from keratinocyte perspective. Cell Death Dis. 2022;13(1):81.
93. Hoegler KM, John AM, Handler MZ, Schwartz RA. Generalized pustular psoriasis: a review and update on treatment. J Eur Acad Dermatol Venereol. 2018;32(10):1645-51.
94. Parisi R, Shah H, Navarini AA, Muehleisen B, Ziv M, Shear NH, et al. Acute Generalized Exanthematous Pustulosis: Clinical Features, Differential Diagnosis, and Management. Am J Clin Dermatol. 2023;24(4):557-75.
95. Brys AK, Rodriguez-Homs LG, Suwanpradid J, Atwater AR, MacLeod AS. Shifting Paradigms in Allergic Contact Dermatitis: The Role of Innate Immunity. J Invest Dermatol. 2020;140(1):21-8.
96. Martin SF. Induction of contact hypersensitivity in the mouse model. Methods Mol Biol. 2013;961:325-35.
97. Rose L, Schneider C, Stock C, Zollner TM, Docke WD. Extended DNFB-induced contact hypersensitivity models display characteristics of chronic inflammatory dermatoses. Exp Dermatol. 2012;21(1):25-31.
98. de Candia P, Prattichizzo F, Garavelli S, Alviggi C, La Cava A, Matarese G. The pleiotropic roles of leptin in metabolism, immunity, and cancer. J Exp Med. 2021;218(5).
99. Souza-Almeida G, Palhinha L, Liechocki S, da Silva Pereira JA, Reis PA, Dib PRB, et al. Peripheral leptin signaling persists in innate immune cells during diet-induced obesity. J Leukoc Biol. 2021;109(6):1131-8.
100. Kiernan K, MacIver NJ. The Role of the Adipokine Leptin in Immune Cell Function in Health and Disease. Front Immunol. 2020;11:622468.
101. Aoki K, Kurashige M, Ichii M, Higaki K, Sugiyama T, Kaito T, et al. Identification of CXCL12-abundant reticular cells in human adult bone marrow. Br J Haematol. 2021;193(3):659-68.
102. Frodermann V, Rohde D, Courties G, Severe N, Schloss MJ, Amatullah H, et al. Exercise reduces inflammatory cell production and cardiovascular inflammation

via instruction of hematopoietic progenitor cells. Nat Med. 2019;25(11):1761-71.

103. De Rosa V, Procaccini C, Cali G, Pirozzi G, Fontana S, Zappacosta S, et al. A key role of leptin in the control of regulatory T cell proliferation. Immunity. 2007;26(2):241-55.

104. Zarkesh-Esfahani H, Pockley AG, Wu Z, Hellewell PG, Weetman AP, Ross RJ. Leptin indirectly activates human neutrophils via induction of TNF-alpha. J Immunol. 2004;172(3):1809-14.

105. Santos-Alvarez J, Goberna R, Sanchez-Margalet V. Human leptin stimulates proliferation and activation of human circulating monocytes. Cell Immunol. 1999;194(1):6-11.

106. Hummel KP, Dickie MM, Coleman DL. Diabetes, a new mutation in the mouse. Science. 1966;153(3740):1127-8.

107. Chen H, Charlat O, Tartaglia LA, Woolf EA, Weng X, Ellis SJ, et al. Evidence that the diabetes gene encodes the leptin receptor: identification of a mutation in the leptin receptor gene in db/db mice. Cell. 1996;84(3):491-5.

108. Bacart J, Leloire A, Levoye A, Froguel P, Jockers R, Couturier C. Evidence for leptin receptor isoforms heteromerization at the cell surface. FEBS Lett. 2010;584(11):2213-7.

109. Constantinescu CS, Farooqi N, O'Brien K, Gran B. Experimental autoimmune encephalomyelitis (EAE) as a model for multiple sclerosis (MS). Br J Pharmacol. 2011;164(4):1079-106.

110. Fujita Y, Fujii T, Mimori T, Sato T, Nakamura T, Iwao H, et al. Deficient leptin signaling ameliorates systemic lupus erythematosus lesions in MRL/Mp-Fas lpr mice. J Immunol. 2014;192(3):979-84.

111. Lourenco EV, Liu A, Matarese G, La Cava A. Leptin promotes systemic lupus erythematosus by increasing autoantibody production and inhibiting immune regulation. Proc Natl Acad Sci U S A. 2016;113(38):10637-42.

112. Amarilyo G, Iikuni N, Shi FD, Liu A, Matarese G, La Cava A. Leptin promotes lupus T-cell autoimmunity. Clin Immunol. 2013;149(3):530-3.

113. De Rosa V, Procaccini C, La Cava A, Chieffi P, Nicoletti GF, Fontana S, et al. Leptin neutralization interferes with pathogenic T cell autoreactivity in autoimmune encephalomyelitis. J Clin Invest. 2006;116(2):447-55.
114. Galgani M, Procaccini C, De Rosa V, Carbone F, Chieffi P, La Cava A, et al. Leptin modulates the survival of autoreactive CD4+ T cells through the nutrient/energy-sensing mammalian target of rapamycin signaling pathway. J Immunol. 2010;185(12):7474-9.
115. Matarese G, Di Giacomo A, Sanna V, Lord GM, Howard JK, Di Tuoro A, et al. Requirement for leptin in the induction and progression of autoimmune encephalomyelitis. J Immunol. 2001;166(10):5909-16.
116. Matarese G, Sanna V, Di Giacomo A, Lord GM, Howard JK, Bloom SR, et al. Leptin potentiates experimental autoimmune encephalomyelitis in SJL female mice and confers susceptibility to males. Eur J Immunol. 2001;31(5):1324-32.
117. Yu Y, Liu Y, Shi FD, Zou H, Matarese G, La Cava A. Cutting edge: Leptin-induced RORgammat expression in CD4+ T cells promotes Th17 responses in systemic lupus erythematosus. J Immunol. 2013;190(7):3054-8.
118. Jakus Z, Simon E, Frommhold D, Sperandio M, Mocsai A. Critical role of phospholipase Cgamma2 in integrin and Fc receptor-mediated neutrophil functions and the effector phase of autoimmune arthritis. J Exp Med. 2009;206(3):577-93.
119. Barlow SM, Morrison PJ, Sullivan FM. Effects of acute and chronic stress on plasma corticosterone levels in the pregnant and non-pregnant mouse. J Endocrinol. 1975;66(1):9O-.
120. Levine S, Treiman DM. Differential Plasma Corticosterone Response to Stress in Four Inbred Strains of Mice. Endocrinology. 1964;75:142-4.
121. Yu N, Qin H, Yu Y, Li Y, Lu J, Shi Y. A Distinct Immature Low-Density Neutrophil Population Characterizes Acute Generalized Pustular Psoriasis. J Invest Dermatol. 2022;142(10):2831-5 e5.
122. Qin B, Yang M, Fu H, Ma N, Wei T, Tang Q, et al. Body mass index and the risk of rheumatoid arthritis: a systematic review and dose-response meta-analysis. Arthritis Res Ther. 2015;17(1):86.

123. Choon SE, Lai NM, Mohammad NA, Nanu NM, Tey KE, Chew SF. Clinical profile, morbidity, and outcome of adult-onset generalized pustular psoriasis: analysis of 102 cases seen in a tertiary hospital in Johor, Malaysia. Int J Dermatol. 2014;53(6):676-84.
124. Williams LM, Campbell FM, Drew JE, Koch C, Hoggard N, Rees WD, et al. The development of diet-induced obesity and glucose intolerance in C57BL/6 mice on a high-fat diet consists of distinct phases. PLoS One. 2014;9(8):e106159.
125. Majewska-Szczepanik M, Kowalczyk P, Marcinska K, Strzepa A, Lis GJ, Wong FS, et al. Obesity aggravates contact hypersensitivity reaction in mice. Contact Dermatitis. 2022;87(1):28-39.
126. Lee M, Lee E, Jin SH, Ahn S, Kim SO, Kim J, et al. Leptin regulates the pro-inflammatory response in human epidermal keratinocytes. Arch Dermatol Res. 2018;310(4):351-62.
127. Murphy EA, Velazquez KT, Herbert KM. Influence of high-fat diet on gut microbiota: a driving force for chronic disease risk. Curr Opin Clin Nutr Metab Care. 2015;18(5):515-20.
128. Sonomoto K, Song R, Eriksson D, Hahn AM, Meng X, Lyu P, et al. High-fat-diet-associated intestinal microbiota exacerbates psoriasis-like inflammation by enhancing systemic gammadelta T cell IL-17 production. Cell Rep. 2023;42(7):112713.
129. Gaudino SJ, Huang H, Jean-Pierre M, Joshi P, Beaupre M, Kempen C, et al. Cutting Edge: Intestinal IL-17A Receptor Signaling Specifically Regulates High-Fat Diet-Mediated, Microbiota-Driven Metabolic Disorders. J Immunol. 2021;207(8):1959-63.
130. Ballesta A, Innominato PF, Dallmann R, Rand DA, Levi FA. Systems Chronotherapeutics. Pharmacol Rev. 2017;69(2):161-99.

9. BIBLIOGRAPHY OF THE CANDIDATE'S PUBLICATIONS

9.1 PUBLICATIONS RELEVANT TO THE THESIS

I. **Bur Z**, Vendl B, Lumniczky Z, Farkas B, Szanto CG, Czaran D, Ella K and Kaldi K

Temporal control of feeding attenuates allergic dermatitis via reduced leptin production in mice

BioRxiv, 2025, doi: 10.1101/2025.10.14.680648

II. **Bur Z**, Vendl B, Sudy AR, Lumniczky Z, Szanto CG, Mocsai A, Kaldi K and Ella K

Time-restricted feeding alleviates arthritis symptoms augmented by high-fat diet.

Front Immunol. 2025, doi: 10.3389/fimmu.2025.1512328

IF: 5.9

III. Ella K, Sudy AR, **Bur Z**, Koos B, Kisiczki AS, Mocsai A and Kaldi K

Time restricted feeding modifies leukocyte responsiveness and improves inflammation outcome.

Front Immunol. 2022, doi: 10.3389/fimmu.2022.924541

IF: 7.3

Cumulative impact factor: 13.2

9.2 PUBLICATIONS UNRELATED TO THE THESIS

I. Bur Z, Ella K
Physiological effects and potential therapeutic application of melatonin
Gyógyszerészet, 2022

II. Bur Z, Ella K
Pharmaceutical implications of the circadian rhythm – From molecular mechanism to chronotherapy
Gyógyszerészet, 2021

10. ACKNOWLEDGEMENTS

I would like to express my deep gratitude to my supervisors, Dr. Krisztina Ella and Dr. Krisztina Káldi, for their trust in welcoming me into their research group both as a TDK and PhD student, guiding me through the early challenges of my research journey. I am deeply thankful for their guidance in my professional development, their dedication to teaching, and for being role models in their passion for science. Their encouragement, kindness, and care created a warm and supportive atmosphere throughout my work.

I am also grateful to Dr. Ágnes Sűdy, who, along with my supervisors, helped me navigate the often challenging path of learning lab work. They introduced me to the fascinating world of experimentation and guided me at the start of my journey in scientific research. I will always value the experiences we shared.

I would like to thank my fellow TDK students and co-authors, including Dr. Bence Koós and Dr. Ármin Kisiczki, for their contributions and the positive energy they brought to our shared experiments and long nights in the lab. Their teamwork truly made all the difference.

Special thanks to my co-author Bernadett Vendl, who was also briefly my co-supervised TDK student. I appreciated the chance to mentor her and share knowledge during that time. Her skillful preparation of the beautiful histological sections from arthritic ankles and inflamed ears truly elevated the quality of our work and made an important contribution to our research. I'm grateful that we can still rely on each other and offer support whenever it's needed.

I am thankful to my co-authors Dr. Zalán Lumniczky and Bianka Farkas, who dedicated tremendous effort and support throughout this project, and to Csongor Szántó for his contribution. Their combined support and reliability meant a great deal, especially during the more challenging times.

I would also like to thank my fellow PhD students, both in and outside the lab: Orsolya Sárkány for her invaluable help within the lab and for being a constant source of encouragement throughout our journey together, as well as Dr. Anita Szőke, who has already completed her PhD, for her support and the many helpful conversations we shared; Dr. Áron Pánczél for always being open to discussing scientific questions and providing valuable methodological insights.

I am grateful to the past and present heads of the Department of Physiology, Prof. László Hunyady and Prof. Attila Mócsai, for making this work possible. I also thank Prof. László Hunyady and Prof. Péter Várnai for their support as doctoral program leaders.

I owe sincere thanks to all members of the Department of Physiology for creating an open, friendly, and professionally inspiring workplace. I am especially grateful to the members of the Ligeti, Mócsai, Geiszt, and Jakus laboratories for their generous help and collaboration on many occasions.

Finally, I am deeply thankful to my family and friends for their love, encouragement, and support. Their patience was just as essential during the many late-night circadian experiments as any other resource.